N76-21181

RESEARCH ON MLS AIRBORNE ANTENNA

Semiannual Report
for period ending November 1975

C. L. Yu and W. D. Burnside

CASE FILE COPY

SEMI-ANNUAL REPORT 2902-23

April 1976

Grant NGL 36-008-138

National Aeronautics and Space Administration
Langley Research Center
Hampton, Virginia 23665

APR 1976
RECEIVED
NASA STI FACILITY
INPUT BRANCH

ABSTRACT

This research program is directed toward the development of numerical solutions for the radiation patterns of antennas mounted on aircraft. It is specifically concerned with the airborne antenna problems associated with the Microwave Landing System (MLS). Based on the requirements of the MLS, volumetric pattern solutions are essential. Previous attempts at solving for the volumetric patterns were found to be far too complex and very inefficient. However as a result of previous efforts, it is possible to combine the elevation and roll plane pattern solutions to give the complete volumetric pattern. This combination is described as well as the aircraft simulation models used in the analysis. A numerical technique is presented to aid in the simulation of the aircraft studied. Finally, a description of the input data used in the computer code is given in the Appendix.

TABLE OF CONTENTS

LIST OF ILLUSTRATIONS

LIST OF ILLUSTRATIONS (continued)

LIST OF ILLUSTRATIONS (continued)

I. INTRODUCTION

All of our work considered during the past year illustrates that numerical solutions for MLS studies provide useful, efficient, and economical evaluation of proposed airborne antenna systems [1] based on their pattern requirements. However, the demands of MLS required a further and more thorough study of ways to handle the complete volumetric pattern. If this problem were to be attacked directly by analyzing rays on complex three-dimensional surfaces as done previously in Ref. [2], the resulting numerical solution would be very complex, time-consuming, and uneconomical. Nevertheless, if certain assumptions are made, the approach undertaken during the past year can be used to overcome these difficulties and simplify the problem a great deal. First, it has been shown by numerous scale model measurements that our roll plane program can be extended to almost cover the complete volumetric pattern except for two conical sectors (fore and aft) [3]. The limitations of the roll plane result are due to the finite length of fuselage. Yet, the finite length fuselage has been solved, previously, through our elevation pattern analyses [4]. Furthermore, based on our previous three-dimensional studies of geodesic rays which contribute to the pattern of an antenna on various prolate spheroids, one is able to combine the analyses of these two principal planes to give the complete pattern. In addition, the cockpit/radome section and stablilizers is taken into account using the flat or bent plate model previously used to analyze the wings in the roll plane. Using this approach, the complete volumetric pattern is obtained using a model consisting of a composite elliptic cylinder to which are attached flat or bent plates. As a result of this simplified model, the program is very efficient and requires little computer storage space. This numerical solution also provides both amplitude and phase data.

This report describes the ways our two previous principal models have been combined together to analyze the complete volumetric pattern in terms of the geometry. The resultant volumetric patterns calculated along with measurement results taken at NASA (Hampton, Va.) are presented to illustrate the validity and capability of our theoretical approach.

II. COMPUTER MODEL OF AN AIRCRAFT

In our study, computer simulation models were considered that would resemble a wide variety of aircraft shapes and yet could, also, be analyzed with reasonable accuracy and economy. In this case, it is quite obvious that the three-dimensional nature of the fuselage must be modeled if one is to adequately determine volumetric patterns. This resulted in the development of a general surface of revolution model of the aircraft fuselage as presented in Ref. [2]. Through an

extensive study of geodesic paths on a general surface of revolution, the number of dominant rays that contribute to the radiation pattern was shown to be finite except for a sphere. Furthermore, the computer result showed that, for a prolate spheroid, the dominant rays needed to be considered would not exceed four rays; in most cases, it is even less than that. These four rays are illustrated in Fig. 1 in which two rays are propagating along the cross-section of the prolate spheroid; the other two are propagating along the profile. To demonstrate the significance of these four rays, the elevation plane

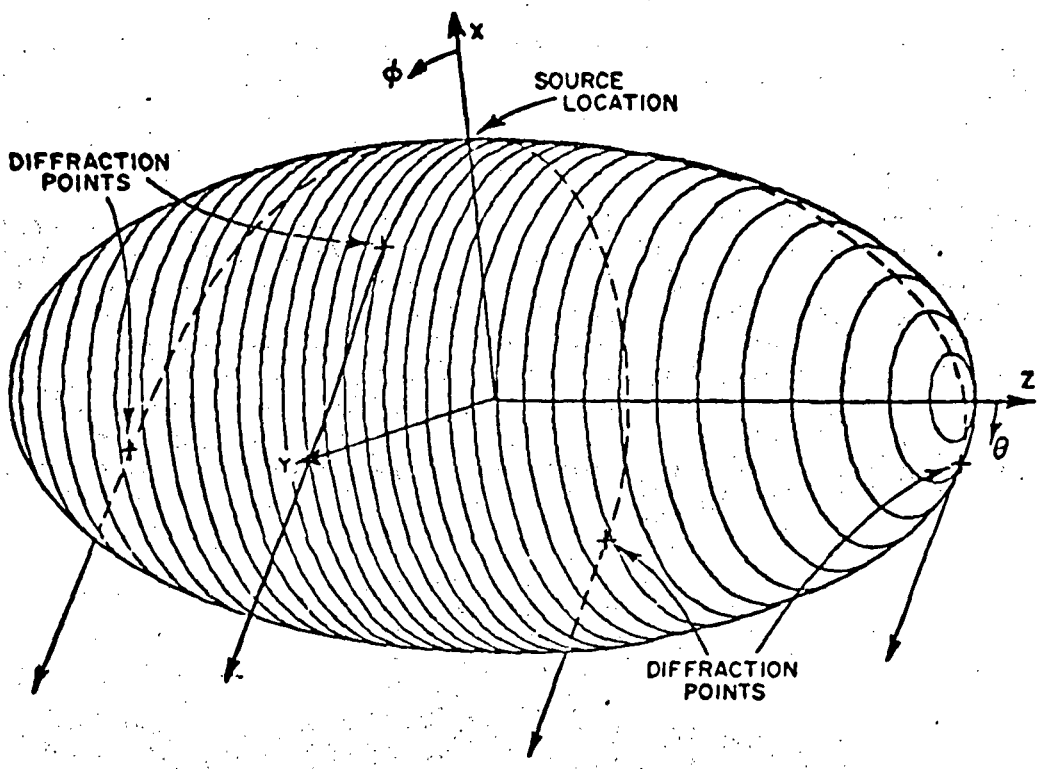

Fig. 1. The four dominant GTD terms that radiate at $\theta = 90°$, $\phi = 145°$).

pattern of an axial slot mounted on a prolate spheroid was calculated using a two-dimensional (two rays) and three-dimensional (four rays) solution as shown in Fig. 2. Experimental results are also shown to verify the calculated three-dimensional result. It is immediately obvious that the back lobe region is not calculated with sufficient accuracy using the two-dimensional result. However, the three-dimensional solution is in good agreement with the measured pattern. This led to a new approach to handle the volumetric patterns for fuselage-mounted airborne antenna in a simplified and economical manner.

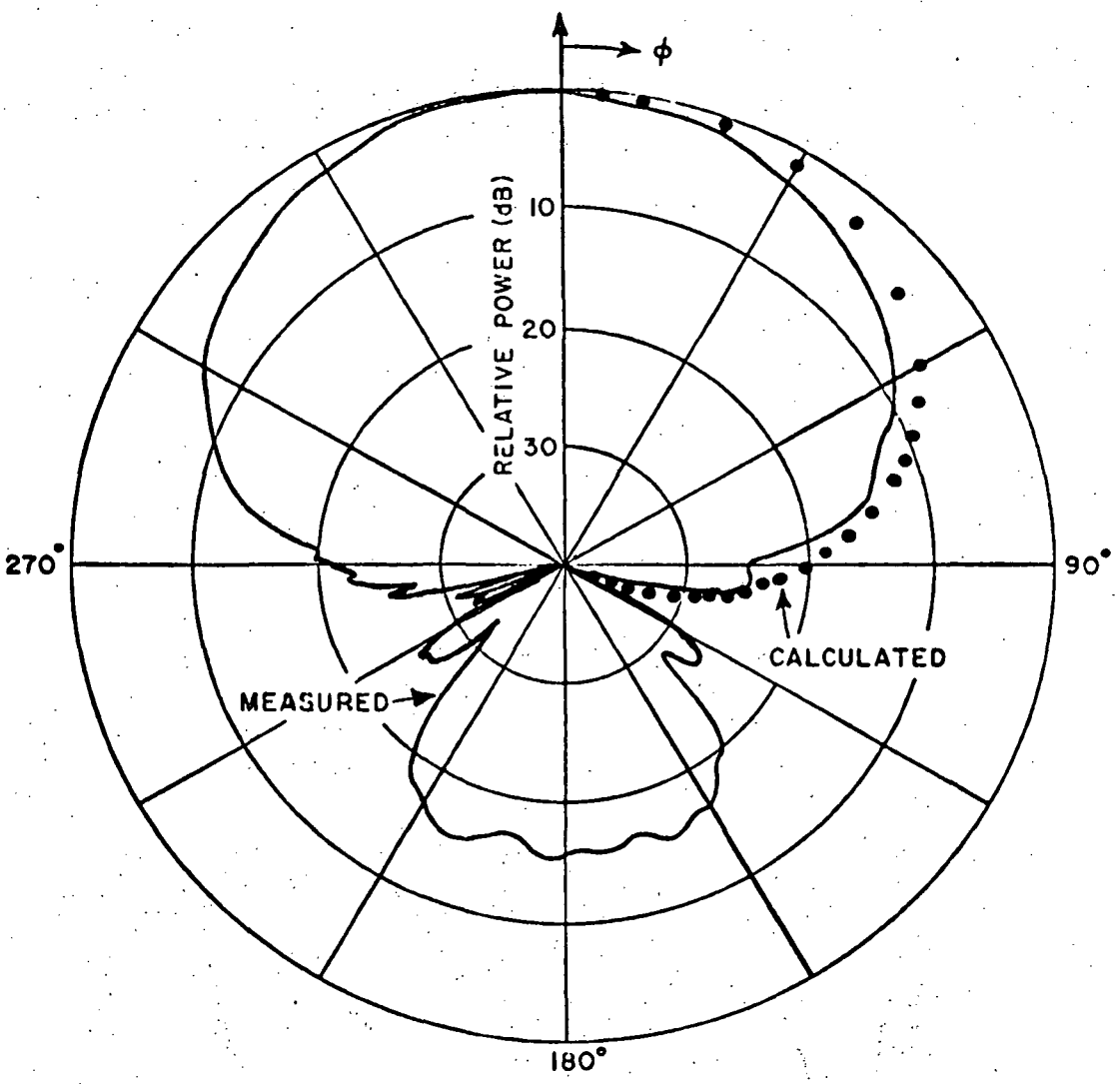

Fig. 2(a). Elevation plane pattern of an axial slot mounted on a 4λ x 2λ prolate spheroid with the two-dimensional theoretical solution presented.

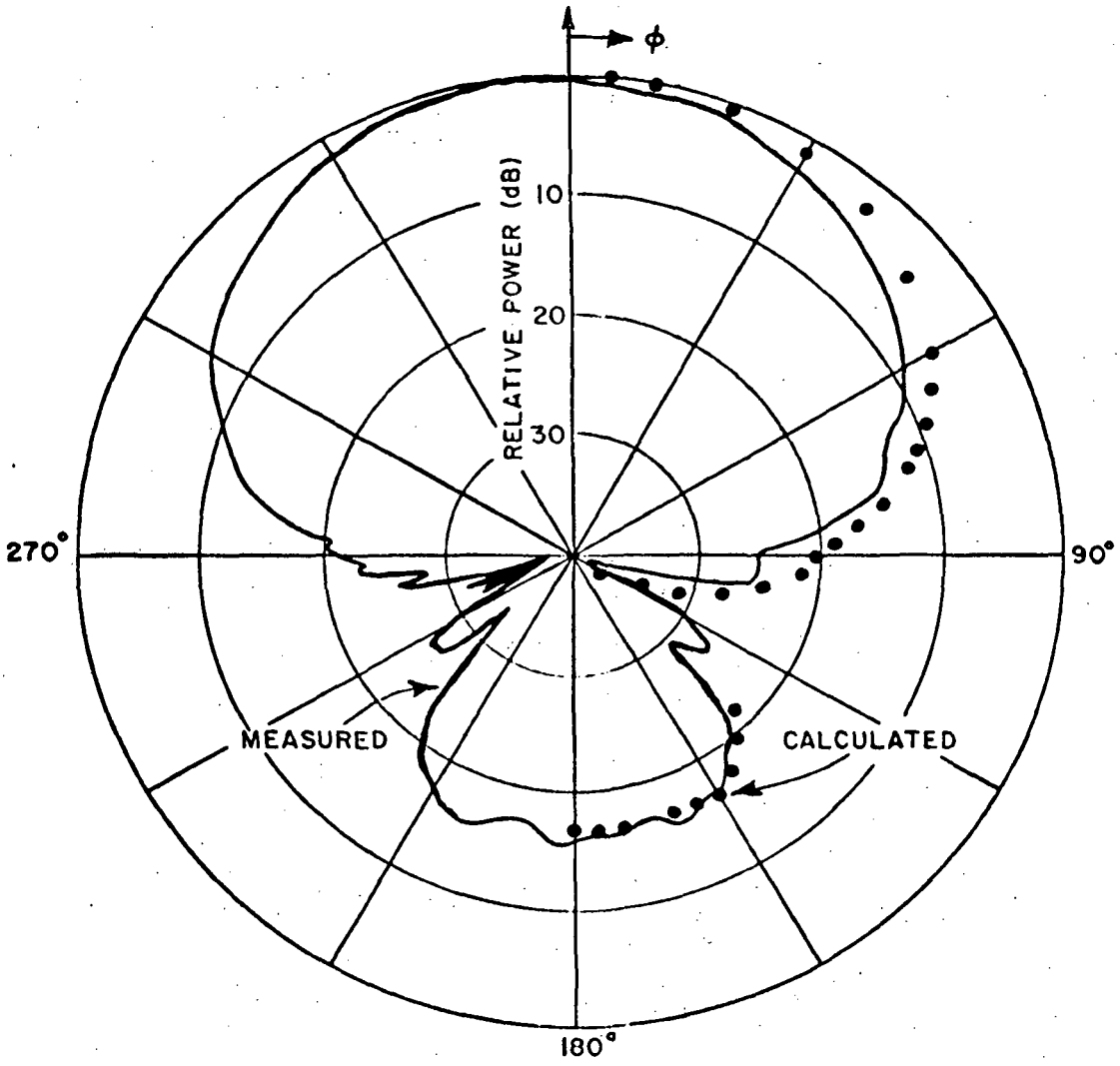

Fig. 2(b). Elevation plane pattern of an axial slot mounted on a 4λ x 2λ prolate spheroid with the three-dimensional theoretical solution presented.

As determined previously, our roll plane program can be extended to cover most of the volumetric pattern except for fore and aft sectors (about 15° conical sector as shown in Fig. 3). To cover these sectors one must incorporate the elevation plane analysis with some modifications such that the effects of wings and stabilizers are also included. In doing so, two different elliptic cylinders are required to analyze the volumetric patterns; one being the cross-section (roll) cylinder and the other being the profile (elevation) cylinder. This requirement is necessary since our solutions are based on infinite elliptic cylinders, in which the z axis coincides with the axis of the cylinder. As discussed in previous work, the most significant effects on the radiation pattern result from the surface geometry nearest to the antenna. The curvature of the curved surface in the vicinity of the antenna location plays a dominant role in predicting the radiation pattern. Thus, the elliptic cylinders which are used to represent the fuselage profile and cross-section should model the aircraft structure as accurately as possible near the antenna location. Once these two elliptic cylinders are obtained, one is able to proceed to solve for the complete volumetric pattern.

The elliptic cylinders necessary to simulate the fuselage profile and cross-section can be found using a best fit routine through the use of a digital computer. A best fit ellipse or composite ellipse is generated through a numerical process by inputting data points that described the surface of the profile or cross-section of the actual aircraft fuselage. Before these data points can be generated, a reference Cartesian coordinates system is needed on a scale model drawing of the aircraft. These coordinates can be best located by aligning one of the axes with the center line of the aircraft fuselage with the origin being aribtrarily chosen according to convenience. After the coordinate system is fixed, the position of data points on the profile or cross-section is measured from the scale model relative to the reference origin. The data points are taken in such a way that more points are needed around the antenna location and less points away from the source. This is due to the fact that the surface profile is dominant near the antenna location as described earlier. Figure 4 illustrates the way data points are taken from the fuselage profile. By feeding these data points into the best fit routine and adjusting the origin of the coordinates in the routine, an ellipse is found to best fit these data points.

The theory behind the best fit routine is that a function is to be found to best approximate a set of points in a least mean square error sense. For our computer model, a best fit ellipse is desired. The mathematical expression for an ellipse is

$$(1) \qquad \frac{x^2}{a^2} + \frac{y^2}{b^2} = 1$$

for its origin located at point (x=0, y=0). The parameters a and b

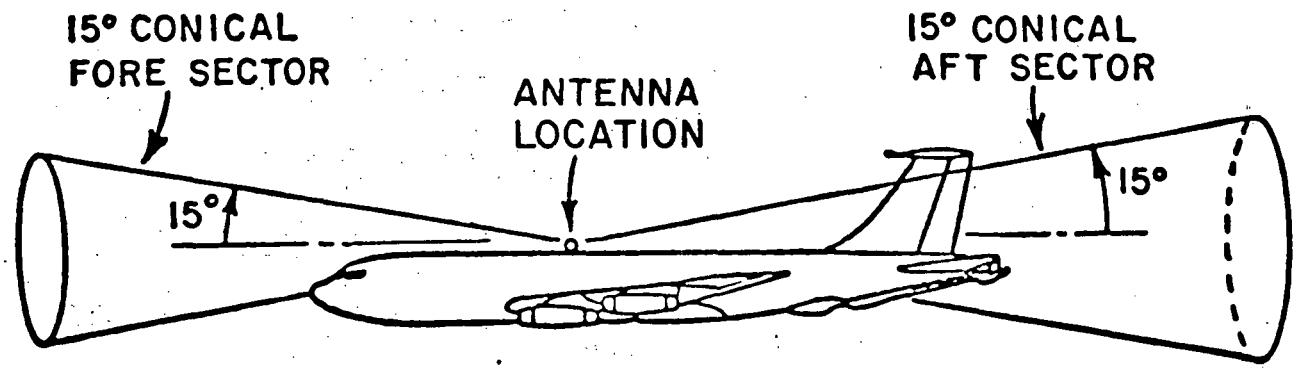

Fig. 3. Fore and aft sectors outside of which our "Roll Plane Model" is valid.

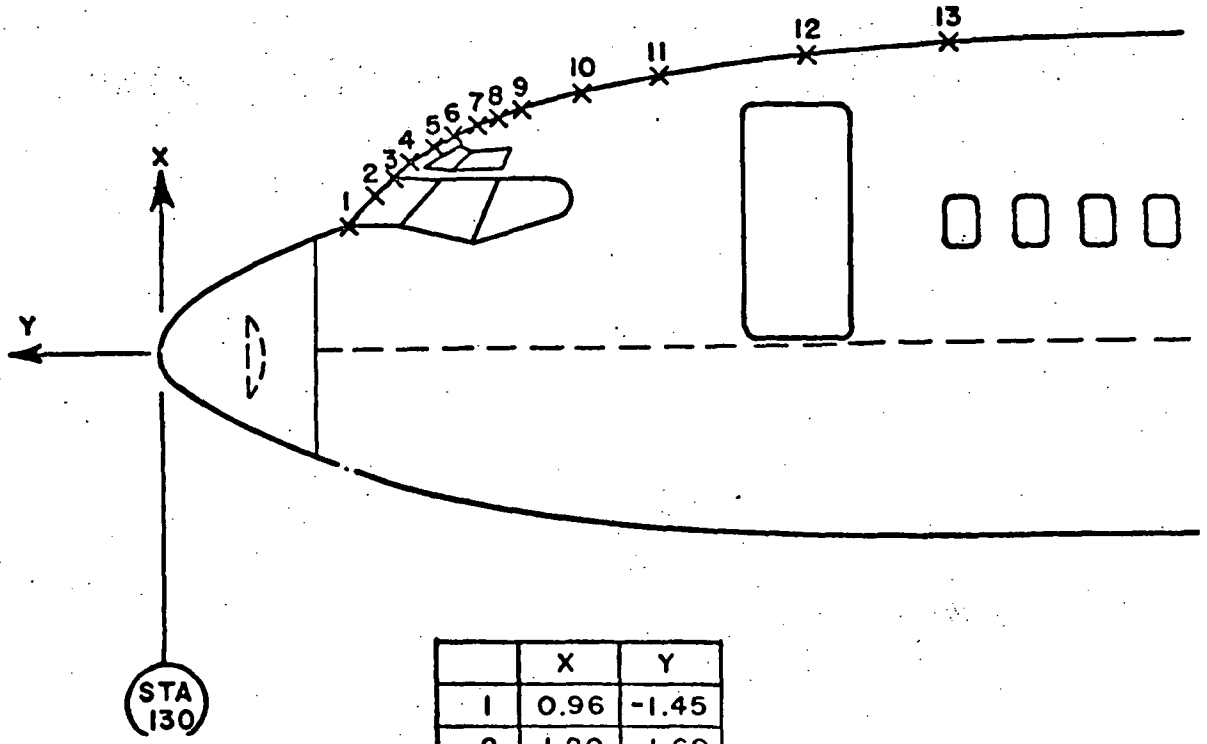

	X	Y
1	0.96	-1.45
2	1.20	-1.69
3	1.34	-1.82
4	1.45	-1.98
5	1.56	-2.16
6*	1.64	-2.30
7	1.69	-2.45
8	1.77	-2.60
9	1.84	-2.80
10	1.98	-3.28
11	2.08	-3.90
12	2.23	-5.01
13	2.30	-6.16
14	2.42	-10.14
15	2.44	-15.72
16	2.28	-24.10

* Antenna Location

Fig. 4. Illustration of data points taken from the scale model aircraft for the determination of best fit elliptic cylinder using a digital computer.

are semi-major and minor axes of an ellipse, respectively. To simplify the mathematical expression, Eq. (1) can be written as

$$AX + BY = 1 \tag{2}$$

where $X = x^2$, $Y = y^2$, $A = \frac{1}{a^2}$, and $B = \frac{1}{b^2}$. Let (x_i, y_i), $i = 1, \cdots n$, be n points from which a best fit ellipse is to be generated. Substituting these points into Eq. (2), one obtains a set of n linear equations.

$$\begin{aligned} AX_1 + BY_1 &= 1 \\ AX_2 + BY_2 &= 1 \\ &\vdots \\ AX_n + BY_n &= 1 \end{aligned} \quad .$$

In matrix form, these n equations become

$$ZC = I \tag{3}$$

where

$$Z = \begin{bmatrix} X_1 & Y_1 \\ X_2 & Y_2 \\ \vdots & \vdots \\ X_n & Y_n \end{bmatrix}$$

$$C = \begin{bmatrix} A \\ B \end{bmatrix}$$

and

$$I = \begin{bmatrix} 1 \\ 1 \\ \vdots \\ 1 \end{bmatrix}$$

By multiplying both sides of Eq. (3) by $\tilde{Z}$, the transposed of Z, one obtains a simple 2x2 matrix as given by

$$\tilde{Z}\, ZC = \tilde{Z}\, I \tag{4}$$

or

$$\begin{bmatrix} \sum_{m=1}^{n} Z_m^2 & \sum_{m=1}^{n} X_m Y_m \\ \sum_{m=1}^{n} X_m Y_m & \sum_{m=1}^{n} Y_m^2 \end{bmatrix} \begin{bmatrix} A \\ B \end{bmatrix} = \begin{bmatrix} \sum_{m=1}^{n} X_m \\ \sum_{m=1}^{n} Y_m \end{bmatrix}$$

which can be simply solved for A and B in the least mean square sense. Thus, the ellipse parameters are defined.

Now let us consider how these two infinite elliptic cylinders can be used to describe the volumetric pattern of fuselage mounted airborne antennas. First, a reference coordinate system is needed so that the solutions, based on our two-dimensional anaysis, in two different coordinate systems can be incorporated into a complete solution. Since an aircraft fuselage is usually long and slender, its finite length effects are limited to the small sectors off the nose and tail. Consequently, the two rays which play the most significant role normally come from the cross-sectional elliptic cylinder. Thus, it seems more natural to have the reference coordinate system correspond to the roll plane coordinate system, i.e., the Z_{ref} axis is pointed aft and the X_{ref} axis is pointed vertically upward as shown in Fig. 5. Recall that the roll plane program is not valid in the two 15° conical sectors in the fore and aft directions. In order to overcome this handicap, a belt region around the antenna source is chosen such that in this region the solution is obtained using the elevation plane analysis. Everywhere outside the belt region, the roll plane analysis is used to analyze the radiation pattern as done previously. The elevation plane results can be incorporated into roll plane solution merely by some coordinate transformations which relate the elevation plane coordinates to the reference coordinate system. As seen in Fig. 5, our elevation plane coordinate system is such that the Z_{elev} axis points in the Y_{ref} direction. In other words, the elevation plane coordinate system is simply obtained by rotating the XYZ_{ref} coordinate system by a 90° angle about the X_{ref} axis. Figure 6 shows the belt region in which elevation plane solution is used. The angle α is chosen such that the roll and elevation solutions blend smoothly together. In fact, α is a function of the size of elevation and roll plane cylinders used to simulate the aircraft fuselage. For most cases in our model, the angle α is set at 20°. This 20° belt has been tested and found to be satisfactory, based on comparisons with measured results.

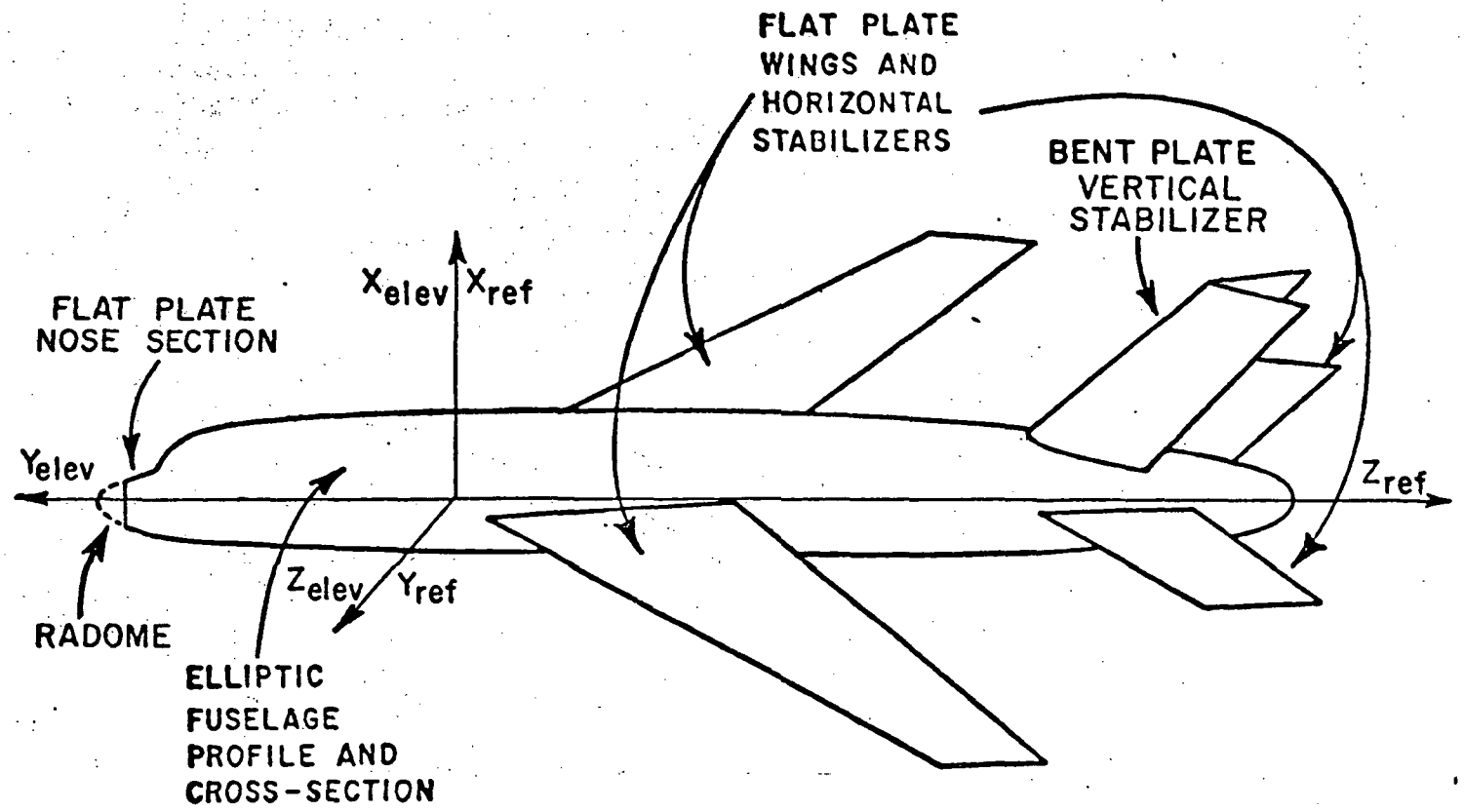

Fig. 5(a). Composite aircraft model and coordinate system illustration.

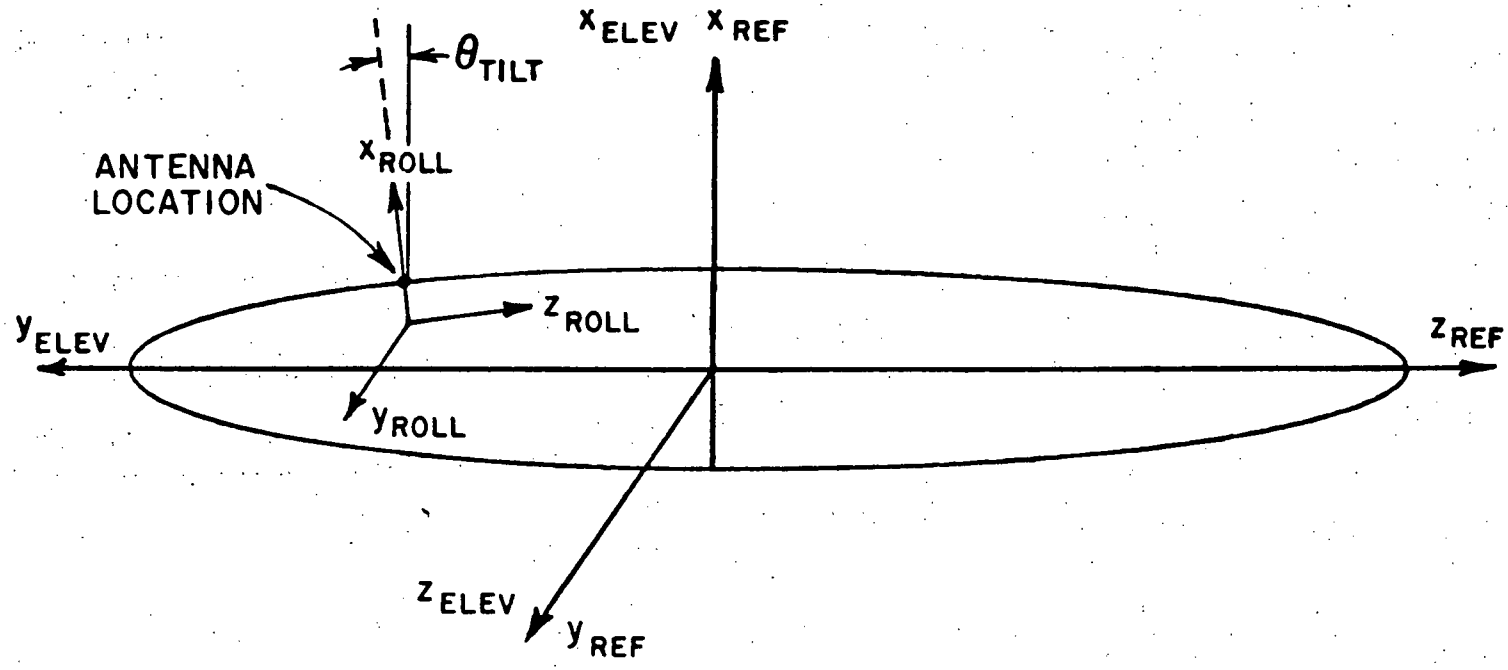

Fig. 5(b). Illustration of various coordinate systems used in our volumetric pattern analysis for center-line mounted antennas.

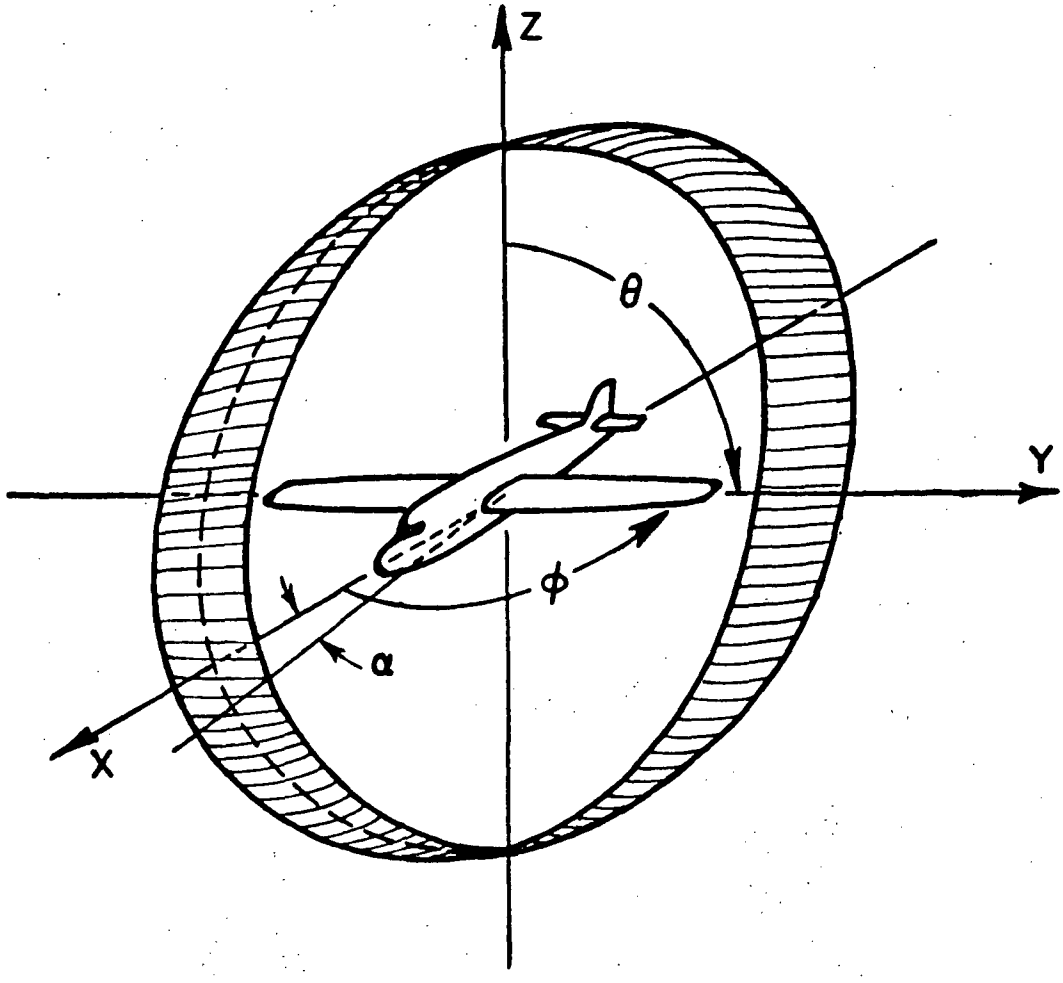

Fig. 6. Illustration of belt region in which elevation plane model analysis is employed.

Recall that four dominant rays contribute to the radiation pattern in the shadow region for an antenna mounted on a prolate spheriod. Since there are only two dominant rays which propagate around an electrically large elliptic cylinder, both elevation and roll plane cylinders are needed to calculate these four rays necessary for the radiation pattern in the shadow region. In addition, the three-dimensional effects of wings and stabilizers are, also, considered everywhere such that the rays reflected and diffracted from these scatters are included. The contributions from the wings and horizontal stabilizers are handled in the same way as done previously [4]. The effect of the cockpit and vertical stabilizer is determined using flat and bent plates attached to the fuselage just at the wings as seen in Fig. 5(b). However, the plates are mounted at arbitrary angles relative to the cylinder in contrast to the restriction of the wings being horizontal presented in the roll plane analysis [4]. In this way, the scattering effects of the cockpit and vertical stabilizer can be taken into account very simply. Finally, the volumetric pattern of fuselage mounted antennas is obtained by summing the direct field from the source and the reflected and diffracted field from the various scatters.

III. RESULT

The theoretical approach to analyze the complete volumetric radiation pattern of fuselage mounted antennas was developed in the last section. The theoretical solution is based on the two principal plane analyses presented earlier [4]. Before it is used to determine the volumetric pattern for an airborne antenna, this recently developed solution must be tested and verified. The elevation pattern of an axial slot mounted on a prolate spheroid, thus, is calculated and presented in Fig. 7. The comparison between the measured and calculated result is very persuasive in that it was shown in Figs. 2(a) and (b) that the three-dimensional effects must be taken into account in order to obtain sufficient accuracy. This particular problem is an effective test in that it illustrates the accuracy for a limiting case that being a small nearly spherical object as opposed to the large cylindrical aircraft model. The aircraft model of most interest in our study is the Boeing 737 aircraft on which extensive experimental and analytical work has been performed.

The computer models used to simulate the Boeing 737 aircraft are shown in Fig. 8, where the roll plane cross-section of the fuselage is approximated by a 65.86"x43.3" elliptic cylinder for an antenna mounted at Station 220 on the top of the fuselage. The elevation profile is modeled by a composite elliptic cylinder with a = 58.72", b = 308.56", and b' = 1307.04". For complete input data refer to Appendix I. Notice that the cockpit is approximated by a finite flat plate. Since computation time in analyzing a real cockpit is so great, it was apparent that a simple model was needed. Originally, a finite bent plate approximation of the cockpit was considered because of the

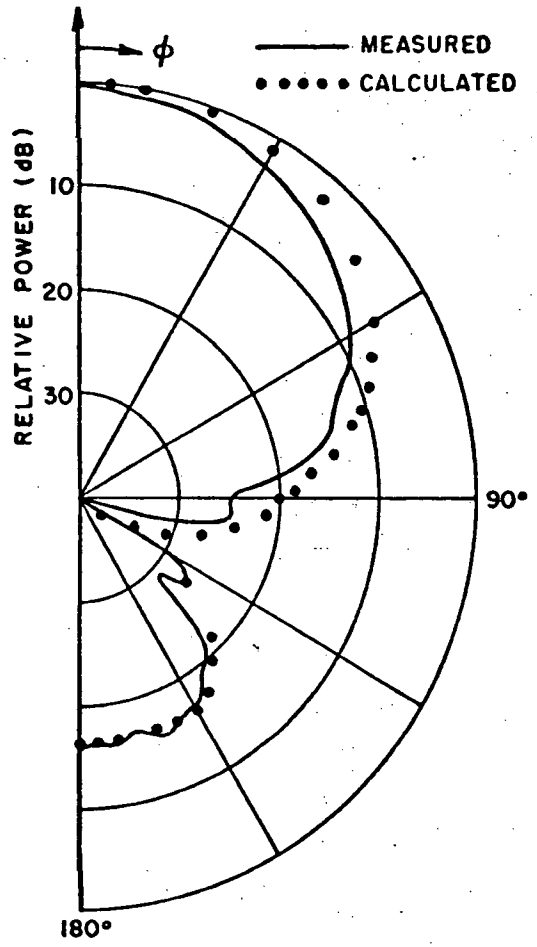

Fig. 7(a). Elevation plane pattern of an axial slot mounted on a 4λ x 2λ prolate spheroid using the surface of revolution approach. (Geometry illustrated in Fig. 1.)

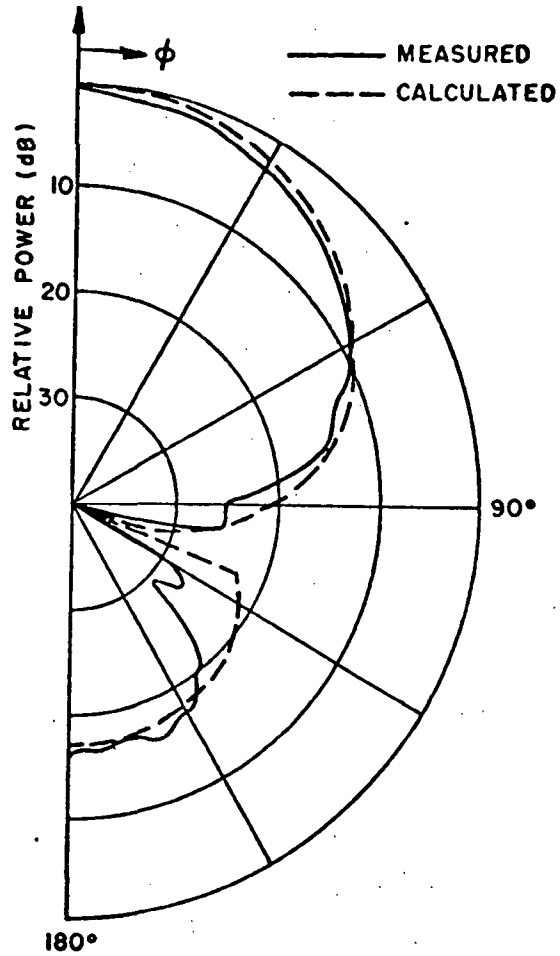

Fig. 7(b). Elevation plane pattern of an axial slot mounted on a 4λ x 2λ prolate spheroid using newly developed volumetric solution. (Geometry illustrated in Fig. 1.)

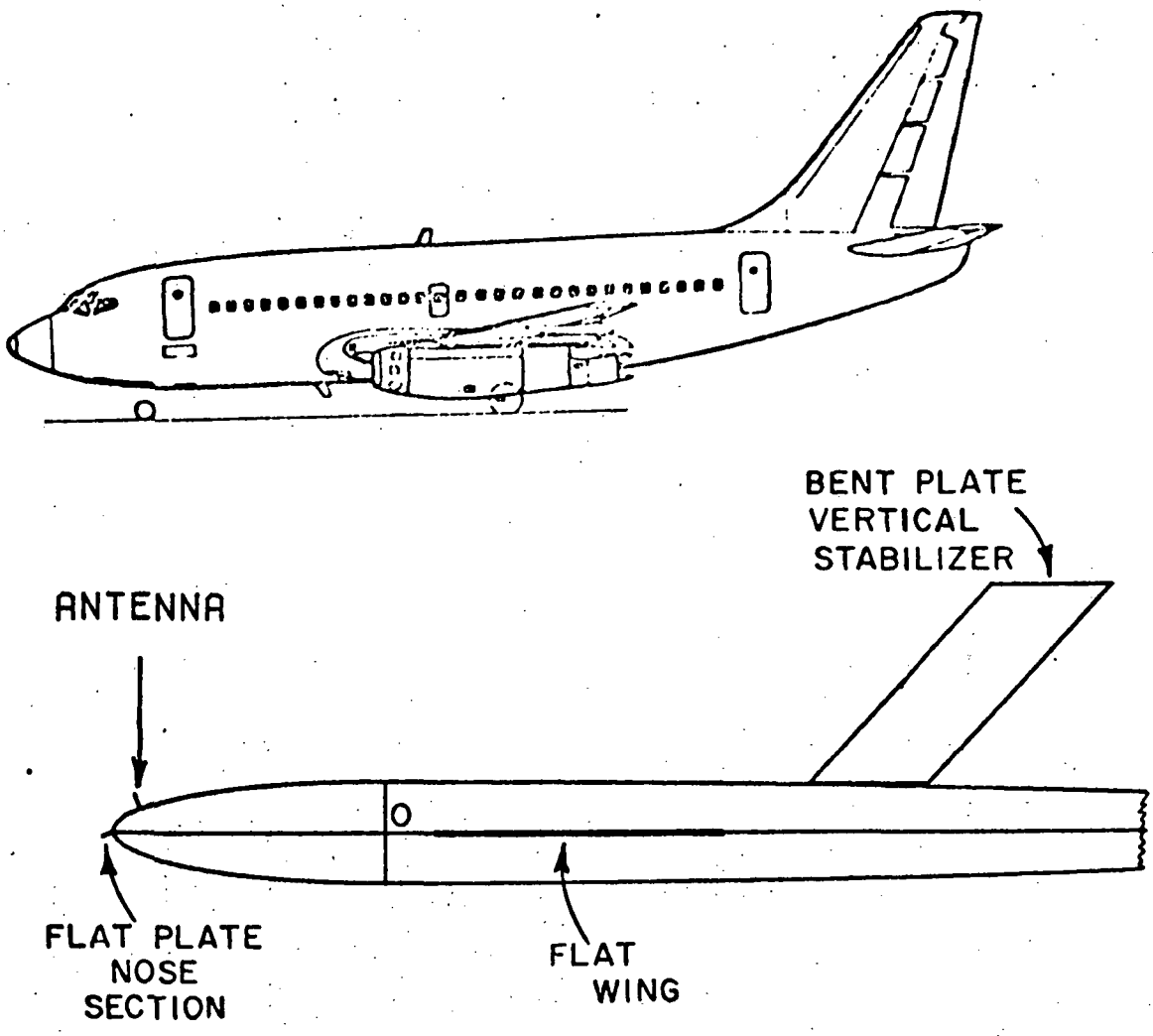

Fig. 8(a). Computer simulated model for the fuselage profile of a Boeing 737 aircraft (side view). The antenna is located at station 220 on top of the fuselage.

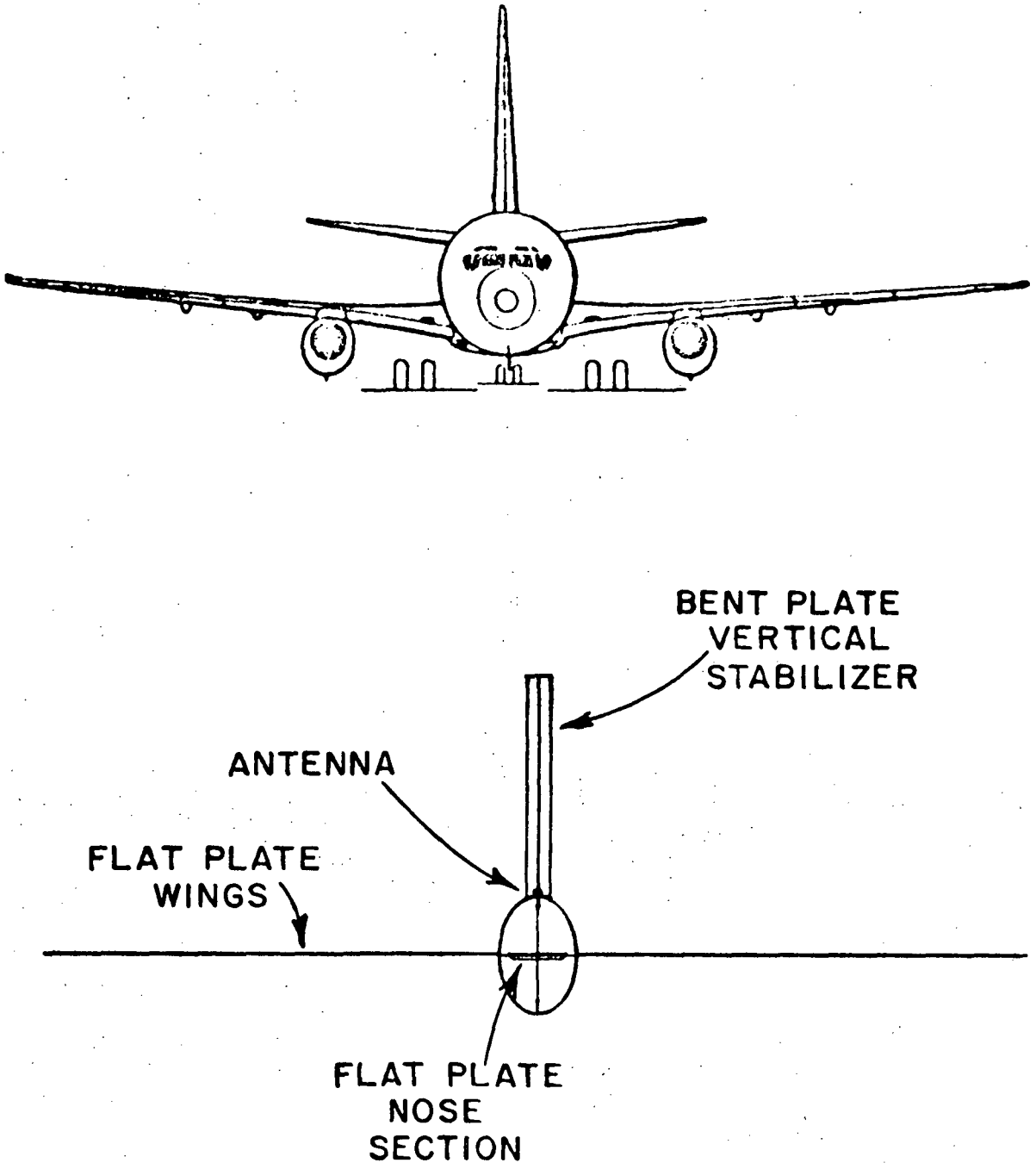

Fig. 8(b). Computer simulated model for the cross-section (at antenna location) of a Boeing 737 aircraft (front view). The antenna is located at station 220 on top of the fuselage.

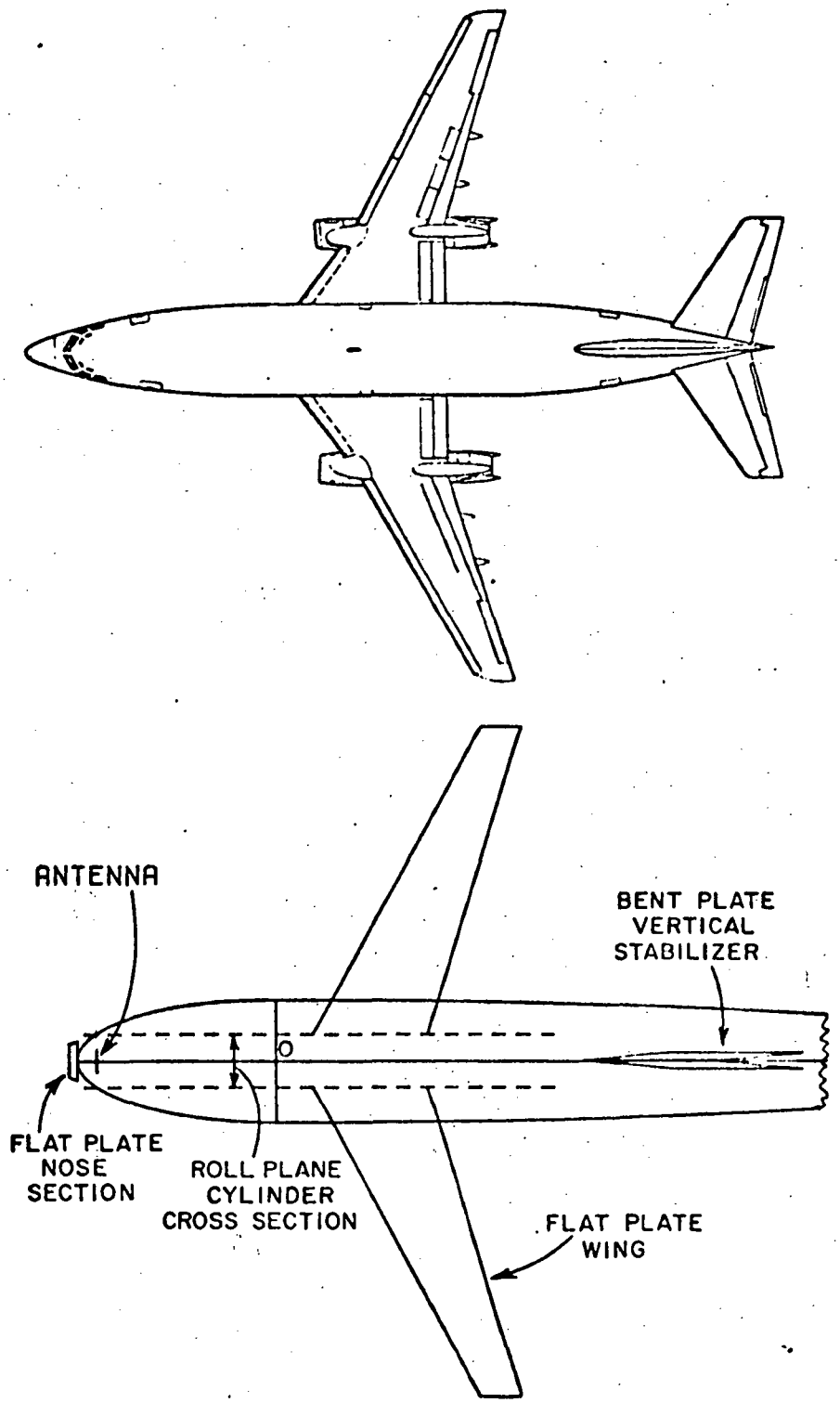

Fig. 8(c). Computer simulated model for a Boeing 737 aircraft (top view). The antenna is located at station 220 on top of the fuselage.

low dielectric constant of the radome. This resulted in a truncated fuselage model as discussed in Ref. [1]. However, the radiation pattern calculated using a flat plate model compared very favorably with the bent plate model. Hence, the flat plate model was adopted not only for its simplicity in analysis but, also, for its reduced computer running time. Similar considerations were made in studying the vertical stabilizer which resulted in a very attractive solution for the aircraft as shown in Fig. 8. The typical roll plane cross-section design is shown in Fig. 8(b). In Fig. 8(c), the top view of our computer model is shown to illustrate the finite three-dimensional effect of an aircraft. The dotted line indicates the width of the cross-sectional (roll plane) cylinder used in the calculation. The geometries of aircraft wings, cockpit, and stabilizers are also presented. The model geometry is taken directly from the three principal views of the aircraft scale model. As presented earlier, the coordinate systems used for both the elevation and roll plane geometries are depicted in Fig. 8.

The radiation patterns for a $\lambda/4$ monopole mounted at Station 220 above the cockpit on a Boeing 737 aircraft are, then, calculated using the computer model just described. The three principal plane results are shown in Figs. 9 to 11 and found to be in very good agreement with measurements. The experimental work was performed with a great deal of patience and precision by the technical staff at NASA (Hampton, Va.). We appreciate their kindness for providing the experimental results for our comparison.

The coordinate system used for the experimental measurements is shown in Fig. 12, in which the z axis is vertically upward. In order to calculate a radiation pattern in terms of this experimental coordinate system, a transformation of coordinates is necessary so that the corresponding radiation direction in our analytical aircraft reference coordinate system can be determined. This is accomplished by considering the z axis of the experimental coordinate system as a radial vector in our reference coordinate system. By inputting its spherical coordinates ($\theta_{Z_{ref}}=90°$, $\phi_{Z_{ref}}=0°$) as the rotation angles θ_c and ϕ_c required in our program, the corresponding radiation direction, in terms of the reference coordinate system, is obtained.

To demonstrate the versatility of our new program, the radiation pattern for an infinitesimal monopole mounted on the bottom side of the fuselage of a Boeing 737 with radome effect included is calculated as shown in Fig. 13(b). The computer model for this case is shown in Fig. 13(a) where the radome effect is simulated by a flat plate mounted vertically upward. This model is adopted because of an experiment investigation of the radome effect which resulted in a truncated fuselage model as discussed in Ref. [1]. Even though double diffractions are not included in the calculation, the resultant pattern is still in very good

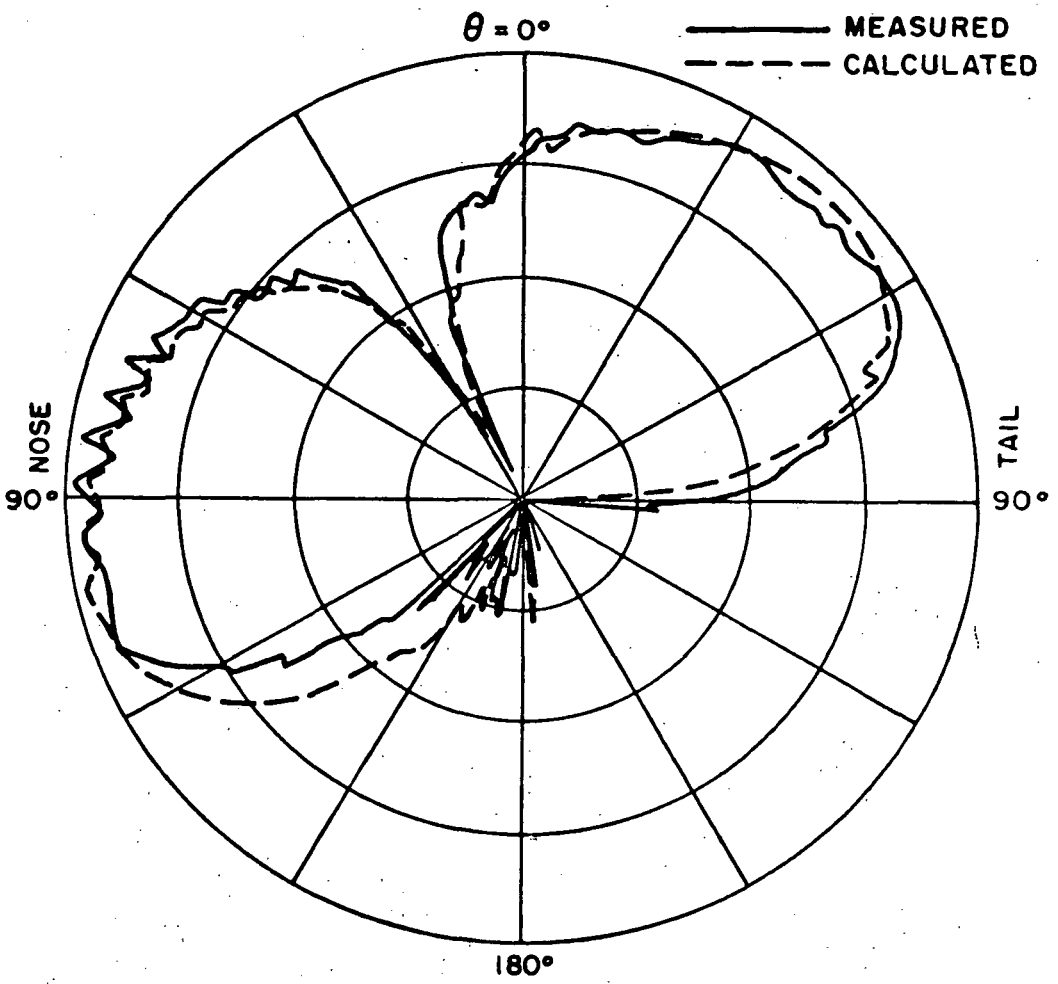

Fig. 9. Elevation plane pattern of a $\lambda/4$ monopole mounted at station 220 on top of a Boeing 737 aircraft. (ϕ = 0° at the left; θ = 180° at the right.)

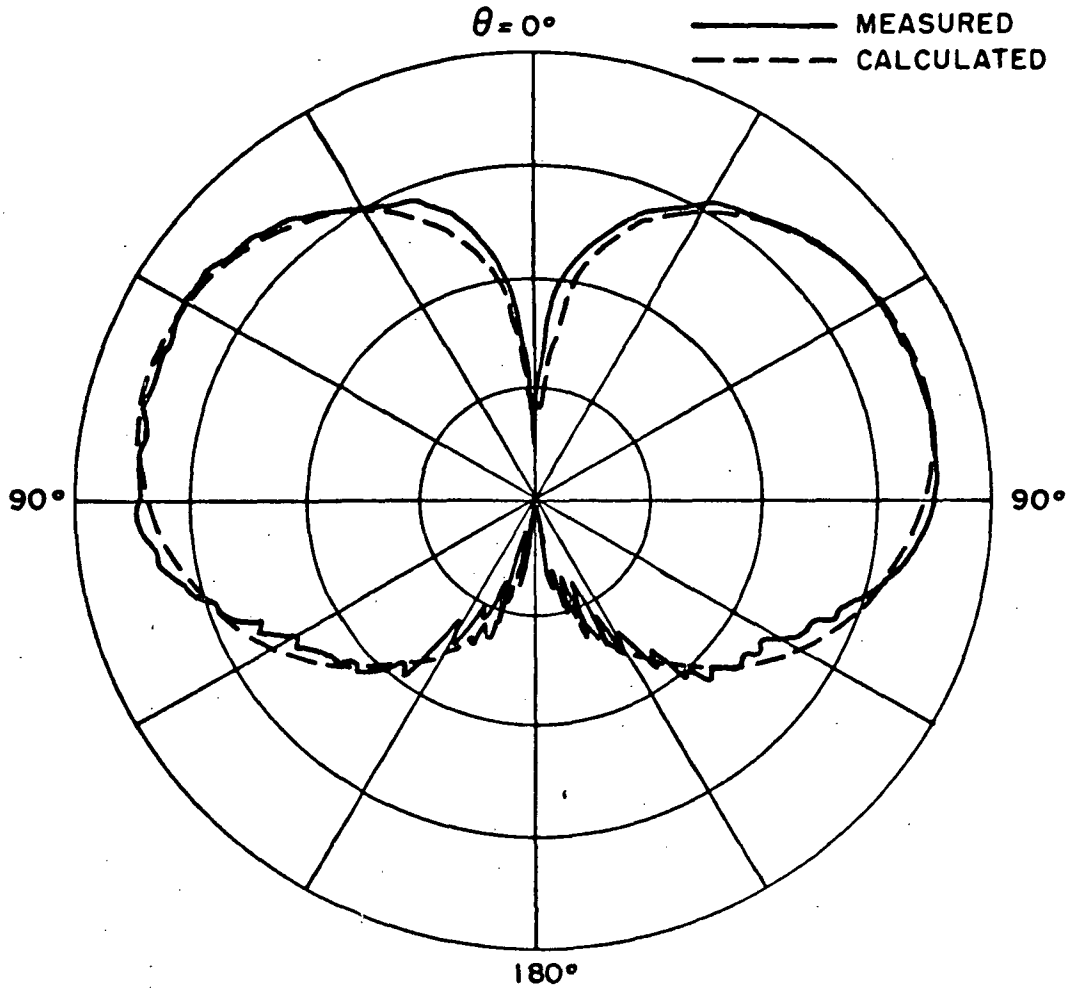

Fig. 10. Roll plane pattern of a $\lambda/4$ monopole mounted at station 220 on top of a Boeing 737 aircraft. (ϕ = 90° at the left; θ = 270° at the right.)

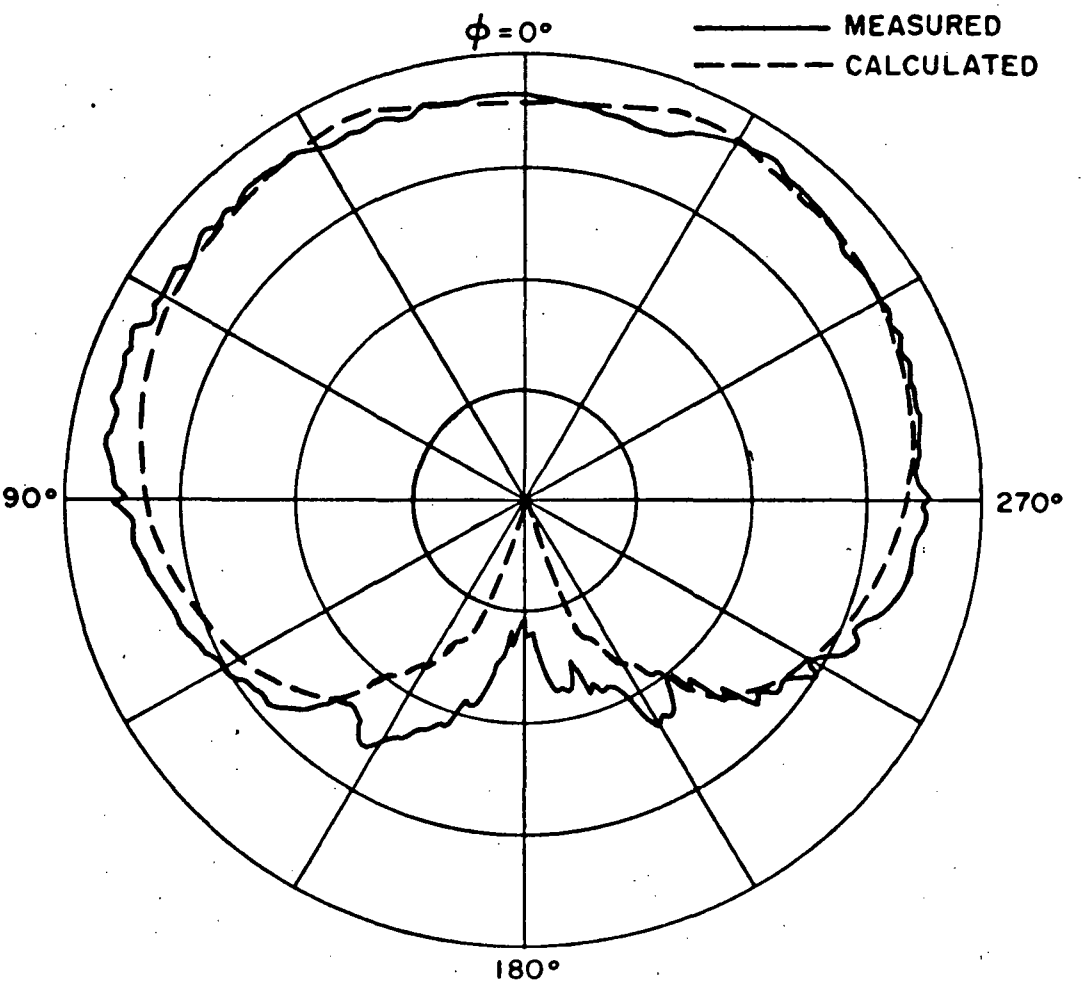

Fig. 11. Azimuth plane pattern of a $\lambda/4$ monopole mounted at station 220 on top of a Boeing 737 aircraft. (θ = 92°.)

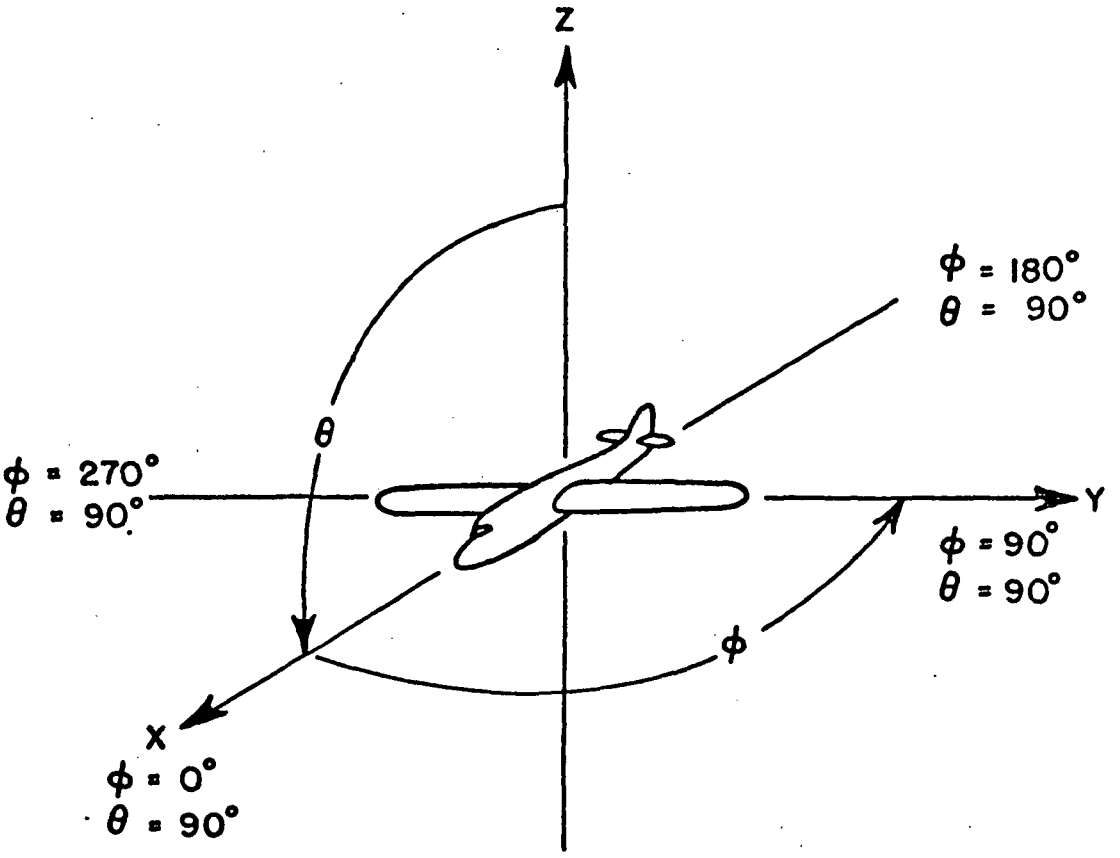

Fig. 12. Illustration of the coordinate system used for experimental measurements.

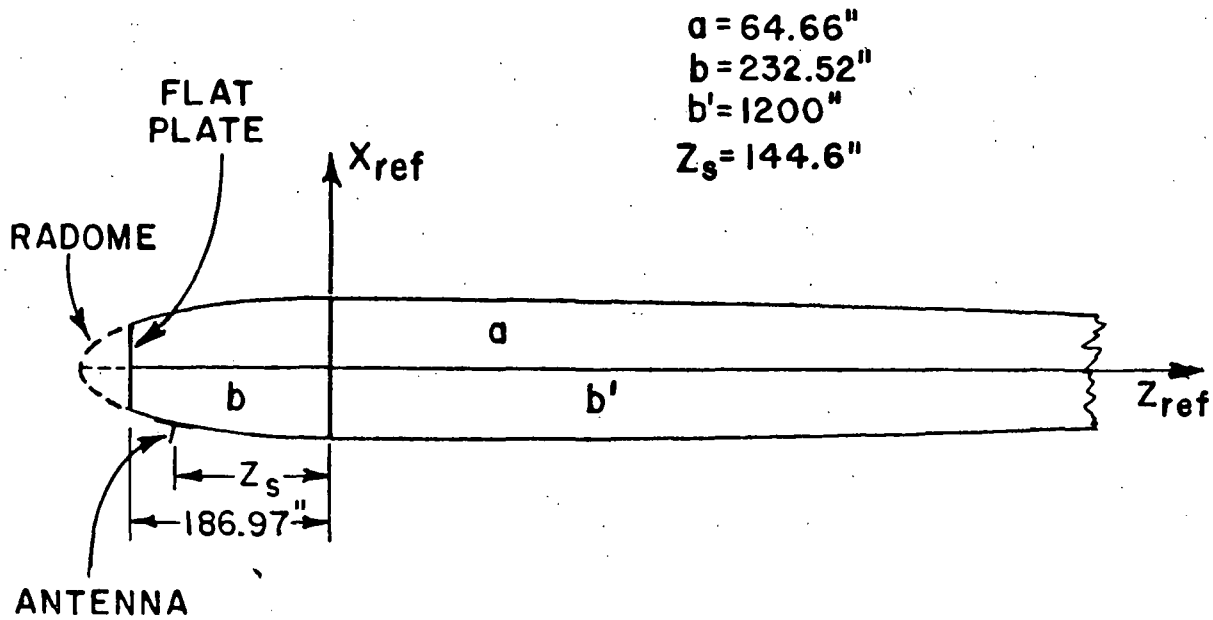

Fig. 13(a). Computer simulated model for a $\lambda/4$ monopole mounted at station 222 on the bottom of the fuselage of a Boeing 737 aircraft (with radome/ nose section being modeled by a flat plate).

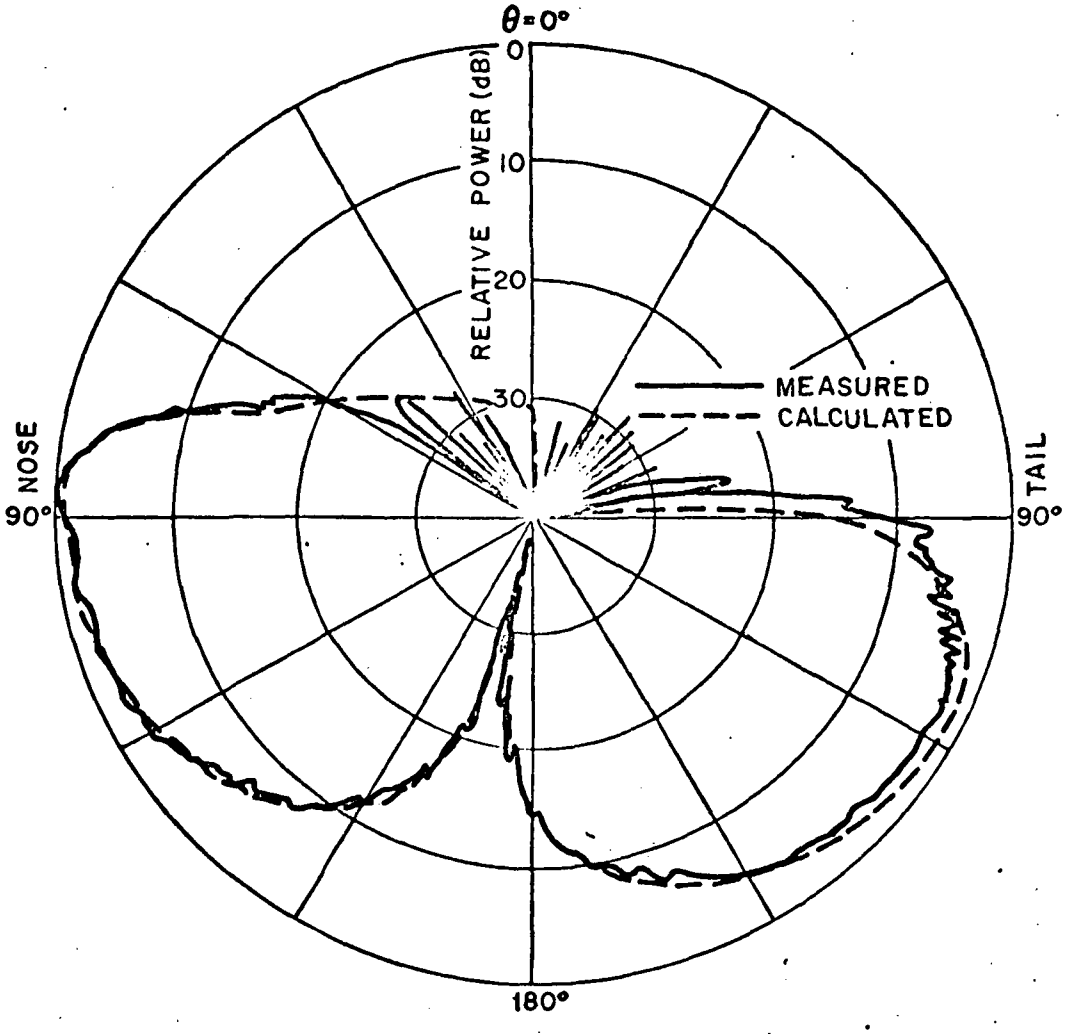

Fig. 13(b). Elevation plane pattern of a $\lambda/4$ monopole mounted at station 222 on the bottom of a Boeing 737 aircraft. (ϕ = 0° at the left; θ = 180° at the right.)

agreement with the measured result. This, again, illustrates the capability of our solution in predicting the radiation pattern of fuselage mounted airborne antennas.

Finally, the complete volumetric pattern for a $\lambda/4$ monopole located at Station 220 on top of a Boeing 737 aircraft is calculated. The off-principal plane elevation patterns are shown in Figs. 14 to 17. The azimuth plane patterns are shown in Figs. 18 to 25. It is noted that the calculated results compare very favorably with the measurements. The various directive gain regions are indicated by the color code. The directive gain, by definition [5], is

$$(5) \qquad G(\theta,\phi) = \frac{\text{radiation intensity } (\theta,\phi)}{\text{average radiated power}} = \frac{4\pi \text{ radiation intensity } (\theta,\phi)}{\text{total radiated power}}$$

The total power radiated by the antenna is obtained by numerically integrating the far field radiation pattern. Using Eq. (5), the gain function is determined for the entire space. The three-dimensional gain pattern is plotted in color as shown in Fig. 26. For example, the pink color indicates the region in space where the gain level is greater than or equal to 0 dB. In other words, this is a region where the radiation intensity of the antenna of interest is greater than that of an isotropic point source. The yellow color indicates the region where the radiation intensity is greater than -3 dB but less than 0 dB in gain level. Consequently, the yellow and pink regions represent the region in space where the gain level of the antenna is equal to or above -3 dB in comparison with an isotropic point source. Similarly, the green, orange, and purple stand for -6 dB, -10 dB, and -15 dB levels in gain, respectively. The experimental results, taken at NASA (Hampton, Va.), are shown in Fig. 27. These patterns represent different gain levels for the antenna under investigation. The comparison between the theoretical and experimental results is seen to be in fairly good agreement. The agreement shown in the gain patterns demonstrates, indeed, the capability of our theoretical solutions in predicting the radiation patterns of airborne antennas mounted on complex aircraft structures. This theoretical calculation not only saves a tremendous amount of expense and manpower, but also the time involved in building a scale model, mounting antennas, and taking the measurements. In addition, the theoretical analysis enables an antenna designer to choose and evaluate the antenna types and locations for the desired coverage for some specific applications in the aircraft design stage. The relocation of an antenna at a future date could also be made easier through this analytical process.

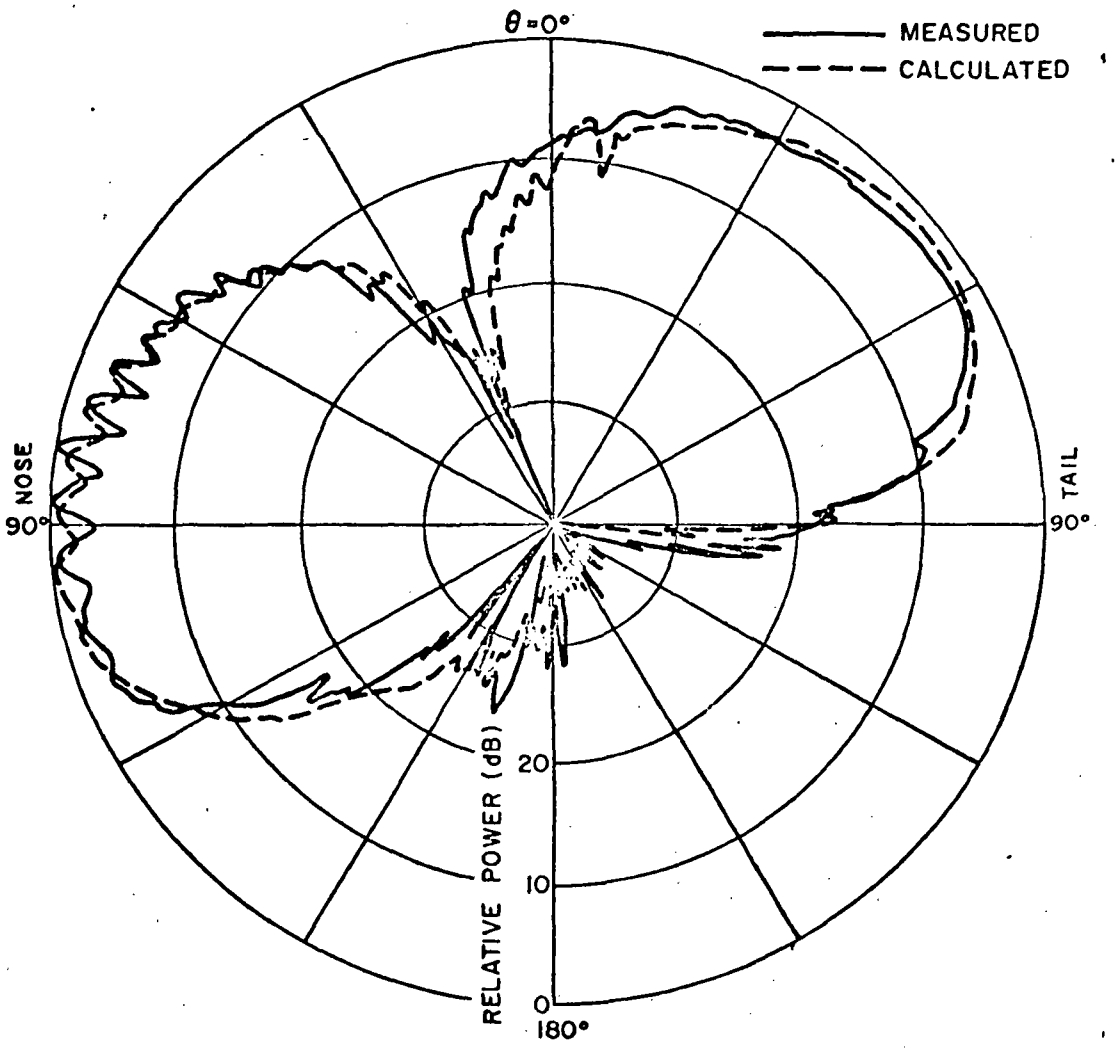

Fig. 14. Elevation plane pattern of a $\lambda/4$ monopole mounted at station 220 on top of a Boeing 737 aircraft. (ϕ = 10° at the left; ϕ = 190° at the right.)

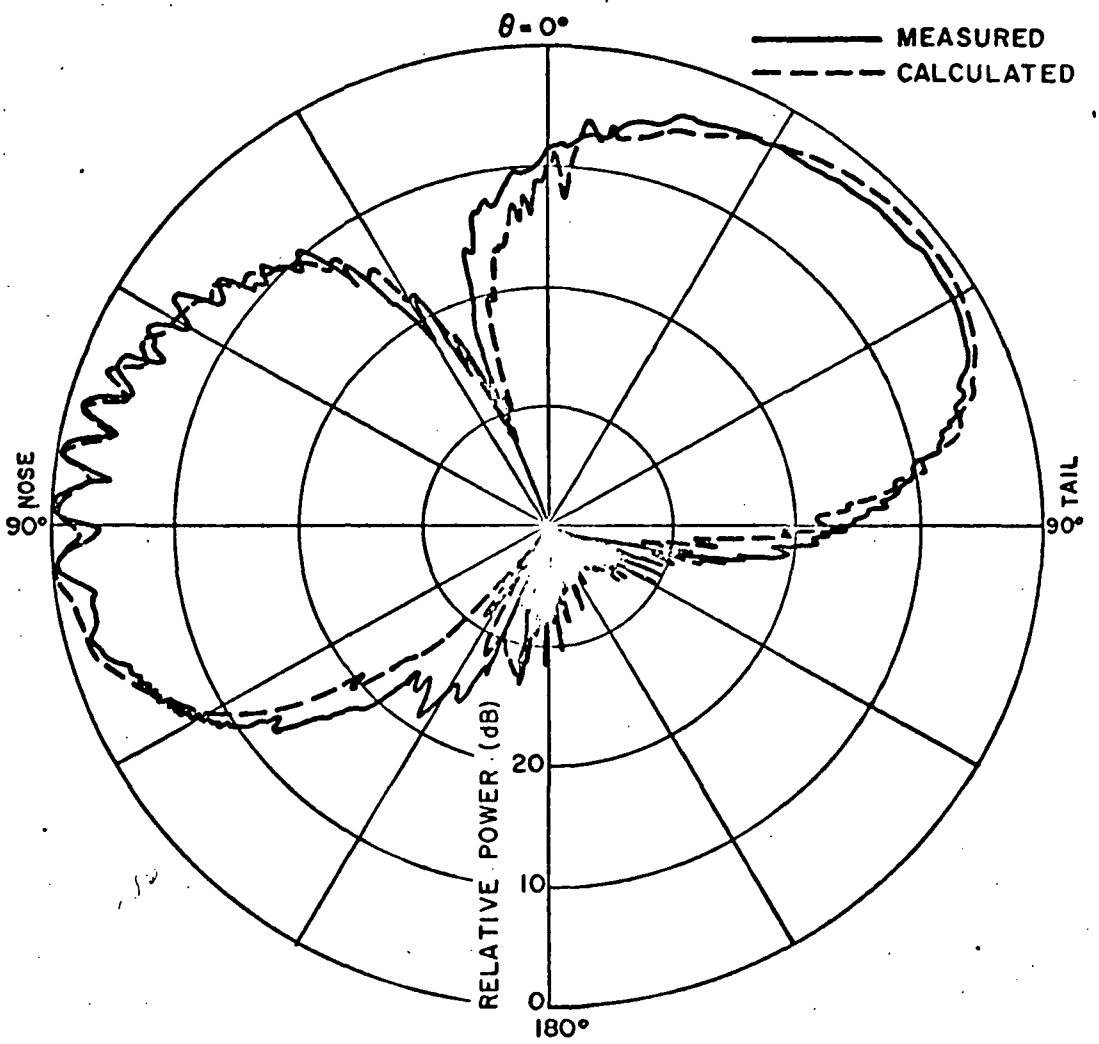

Fig. 15. Elevation plane pattern of a $\lambda/4$ monopole mounted at station 220 on top of a Boeing 737 aircraft. (ϕ = 20° at the left; ϕ = 200° at the right.)

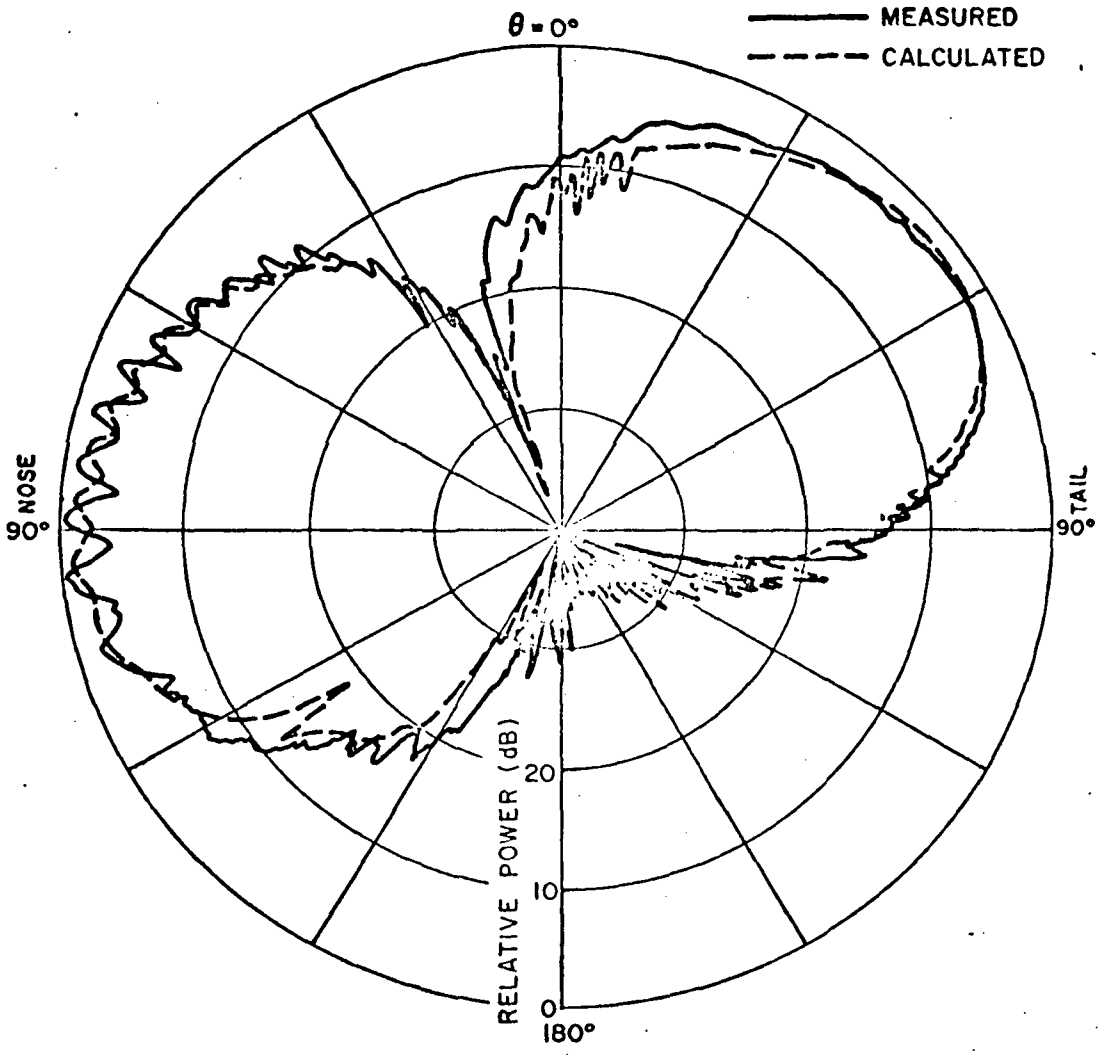

Fig. 16. Elevation plane pattern of a $\lambda/4$ monopole mounted at station 220 on top of a Boeing 737 aircraft. (ϕ = 30° at the left; ϕ = 210° at the right.)

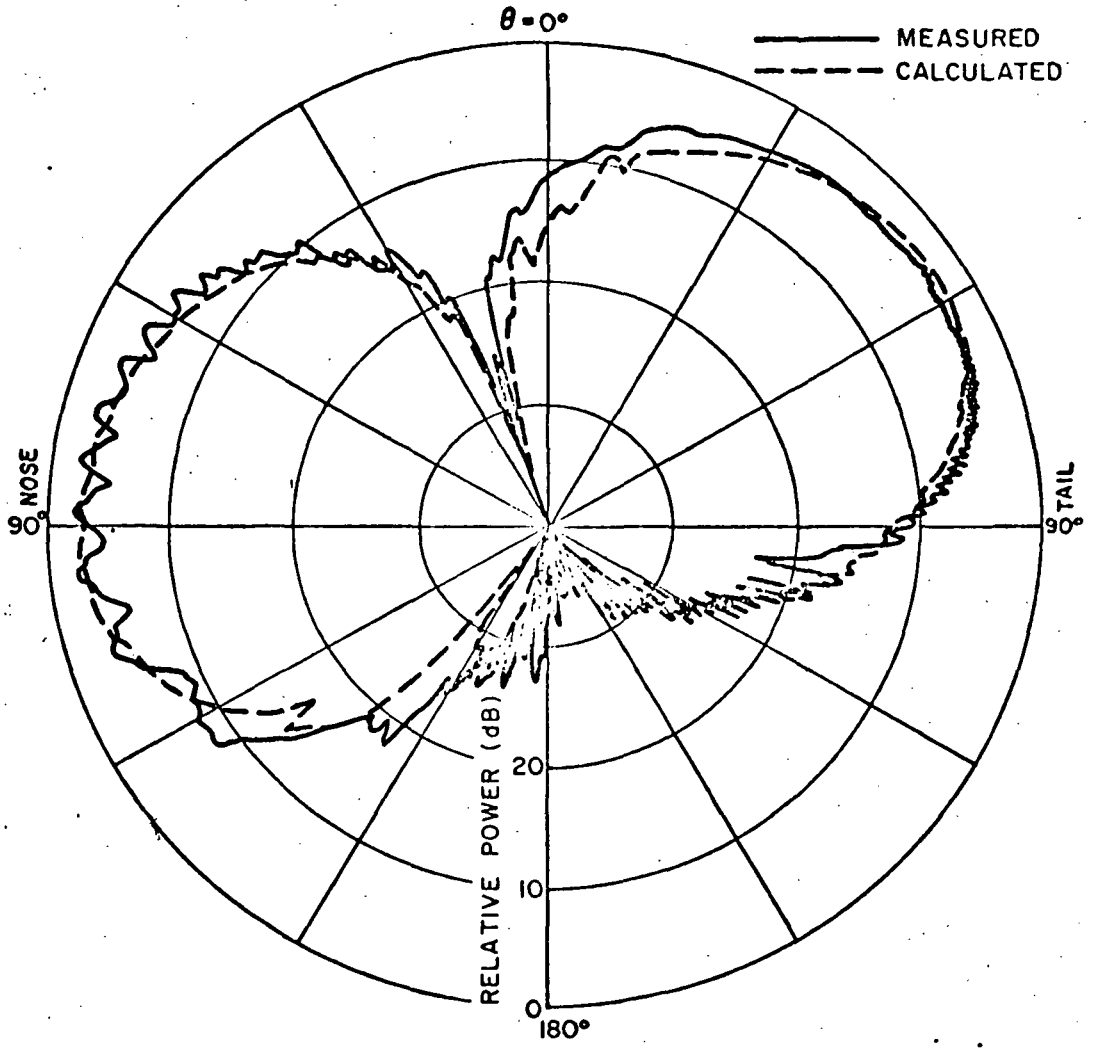

Fig. 17. Elevation plane pattern of a $\lambda/4$ monopole mounted at station 220 on top of a Boeing 737 aircraft. (ϕ = 40° at the left; ϕ = 220° at the right.)

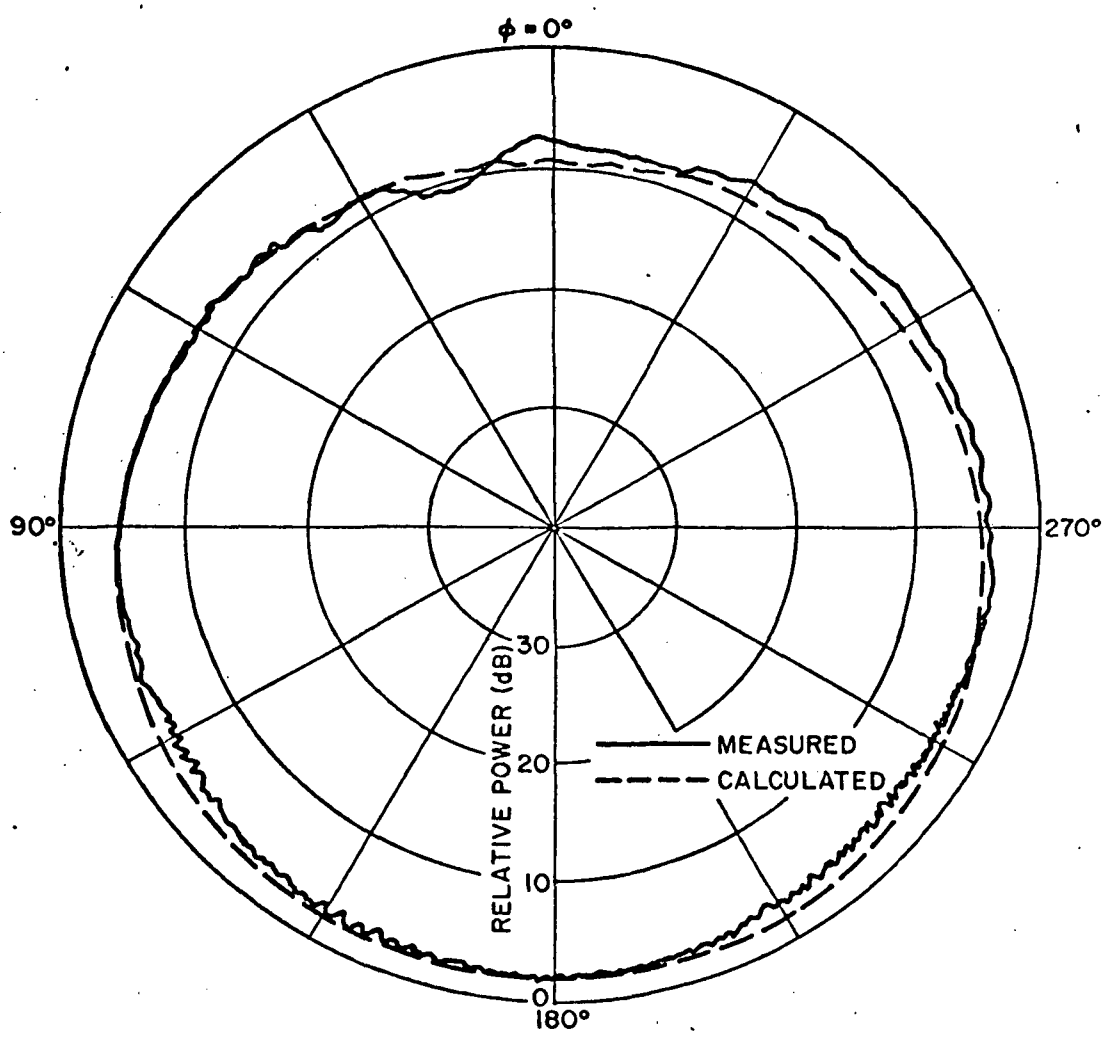

Fig. 18. Azimuth plane pattern of a λ/4 monopole mounted at station 220 on top of a Boeing 737 aircraft. (θ = 50°.)

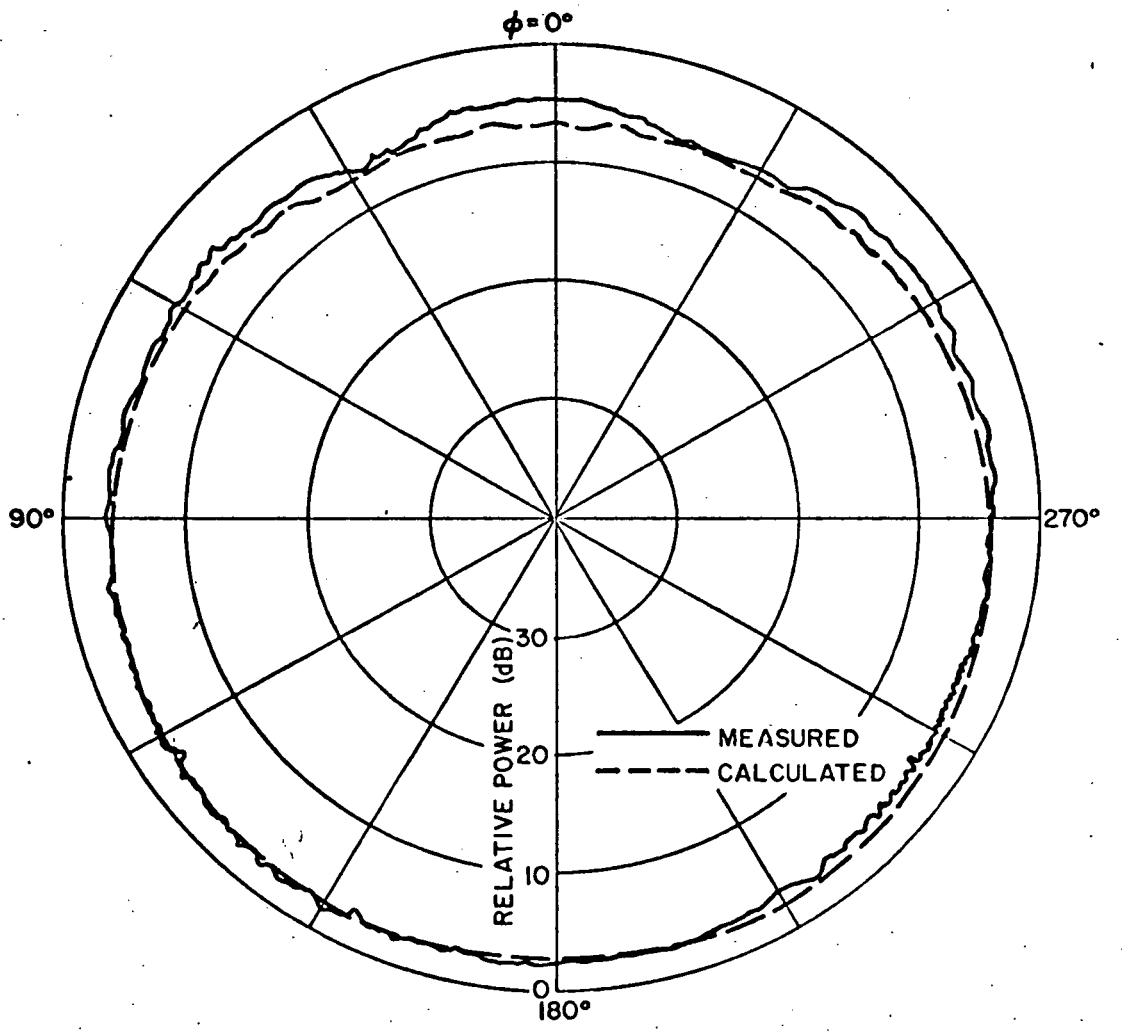

Fig. 19. Azimuth plane pattern of a λ/4 monopole mounted at station 220 on top of a Boeing 737 aircraft. (θ = 60°.)

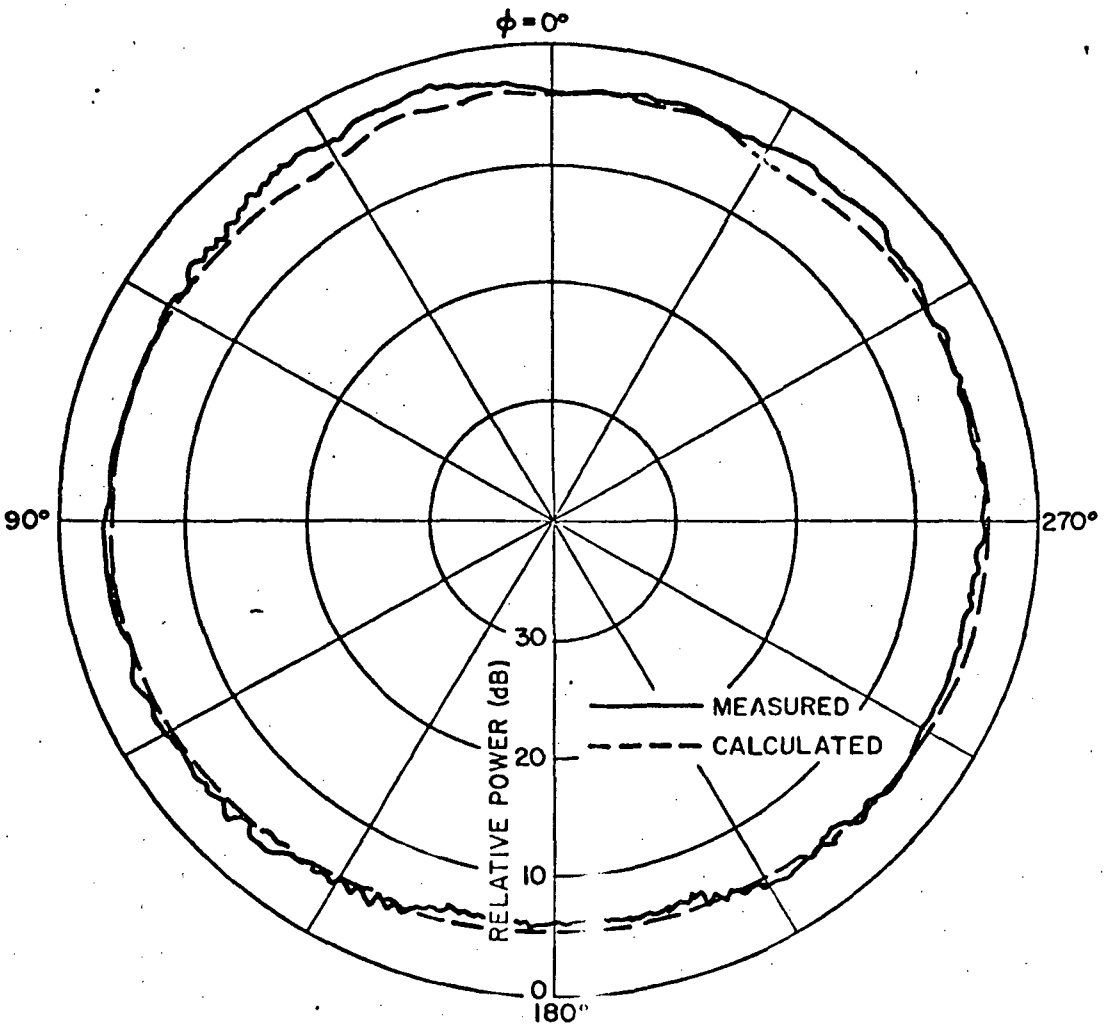

Fig. 20. Azimuth plane pattern of a λ/4 monopole mounted at station 220 on top of a Boeing 737 aircraft. (θ = 70°.)

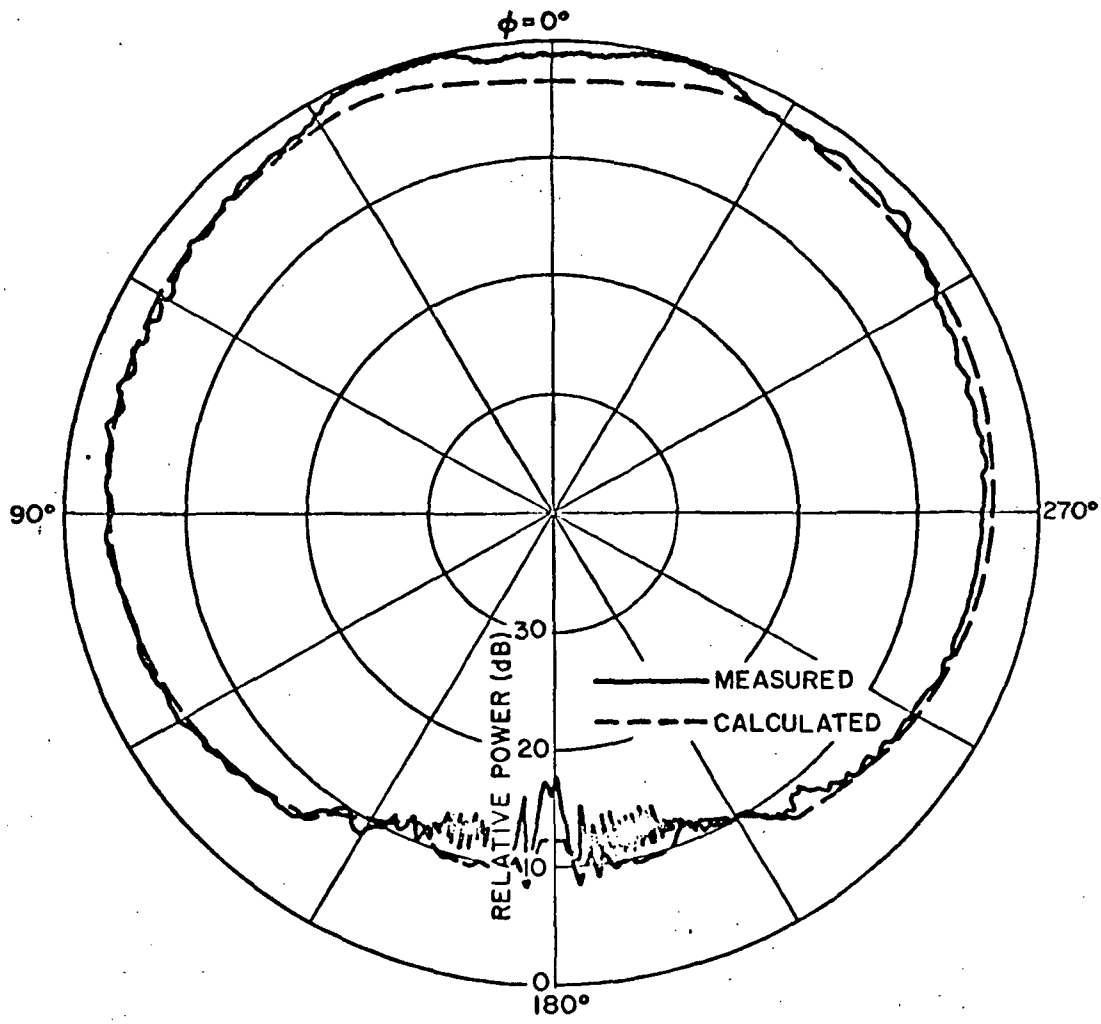

Fig. 21. Azimuth plane pattern of a $\lambda/4$ monopole mounted at station 220 on top of a Boeing 737 aircraft. (θ = 80°.)

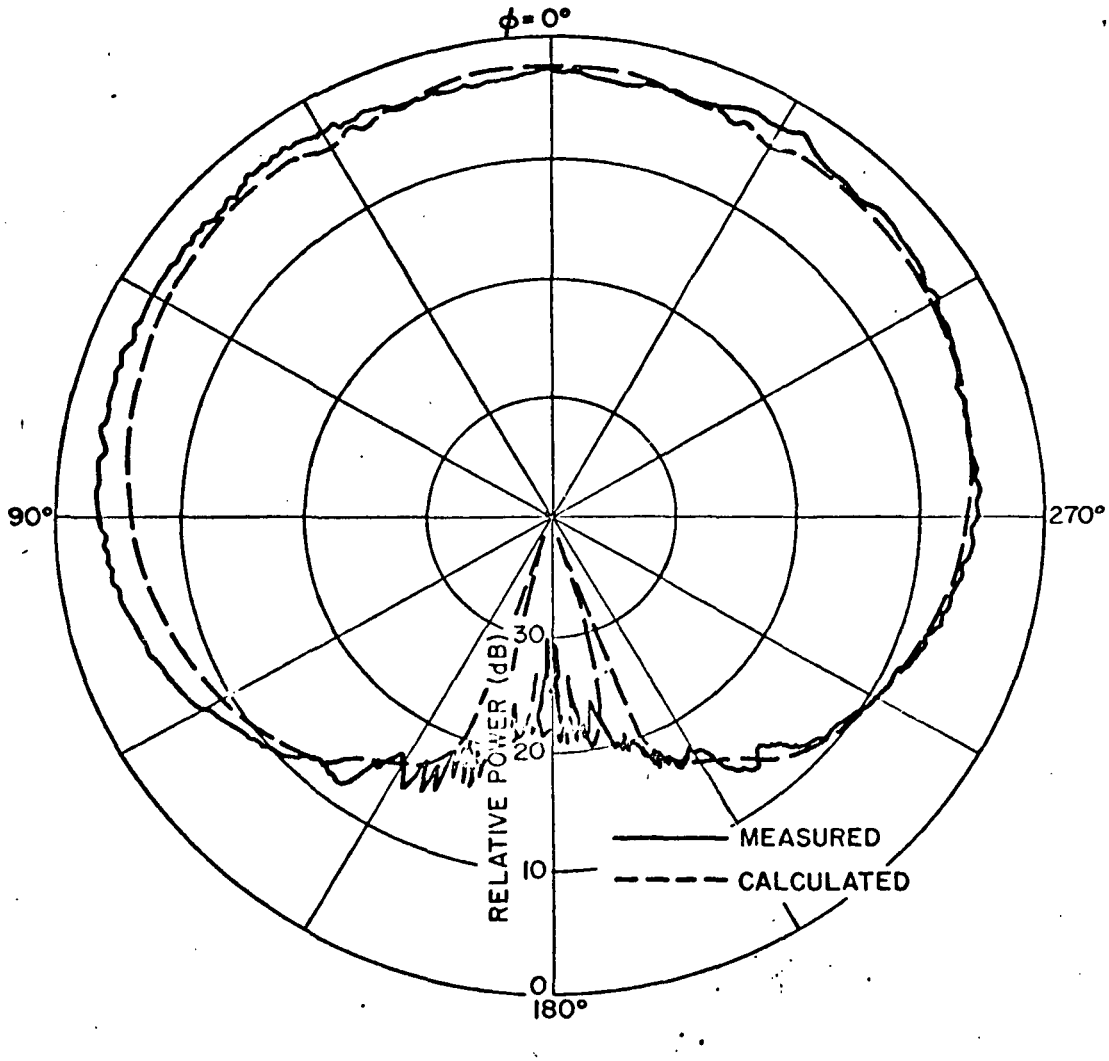

Fig. 22. Azimuth plane pattern of a $\lambda/4$ monopole mounted at station 220 on top of a Boeing 737 aircraft. (θ = 90°.)

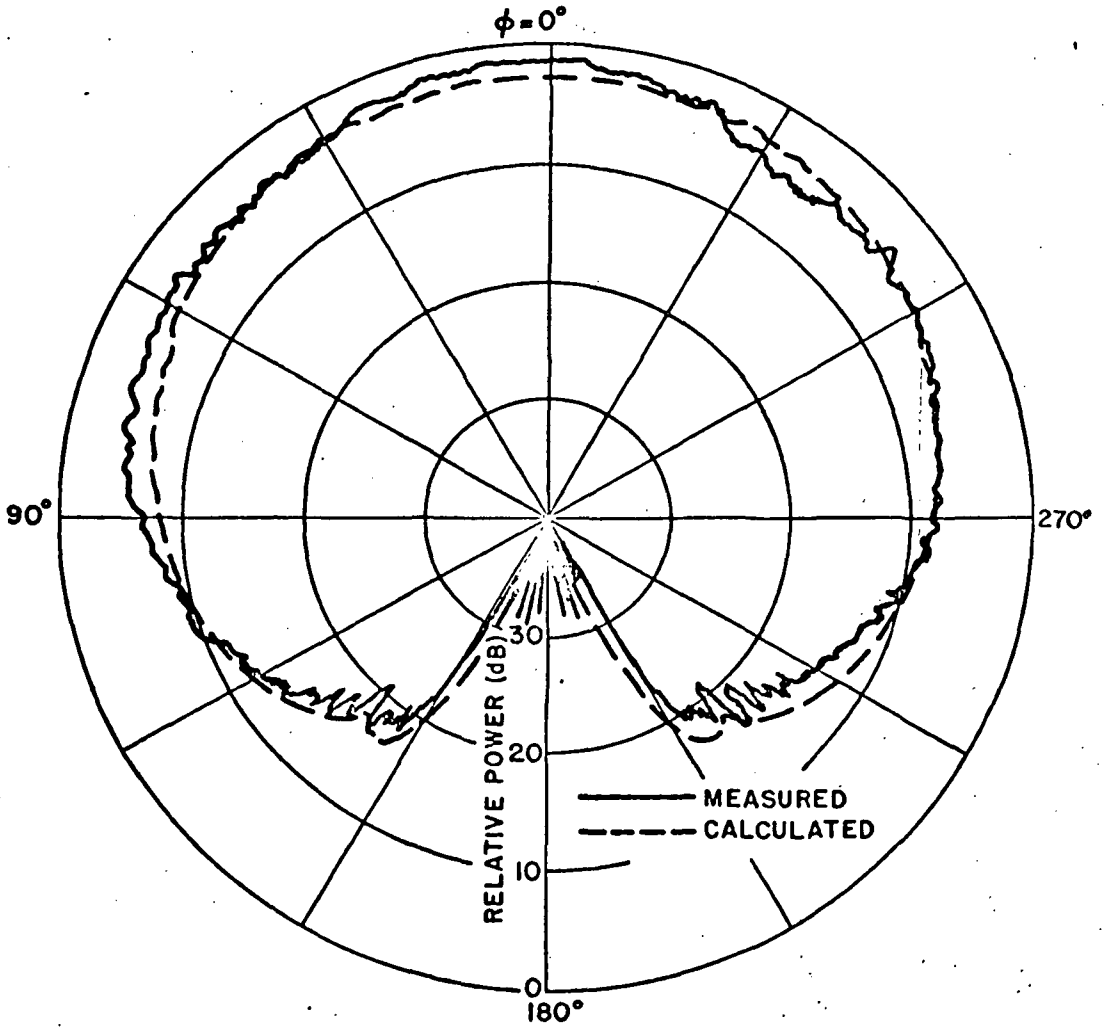

Fig. 23. Azimuth plane pattern of a λ/4 monopole mounted at station 220 on top of a Boeing 737 aircraft. (θ = 100°.)

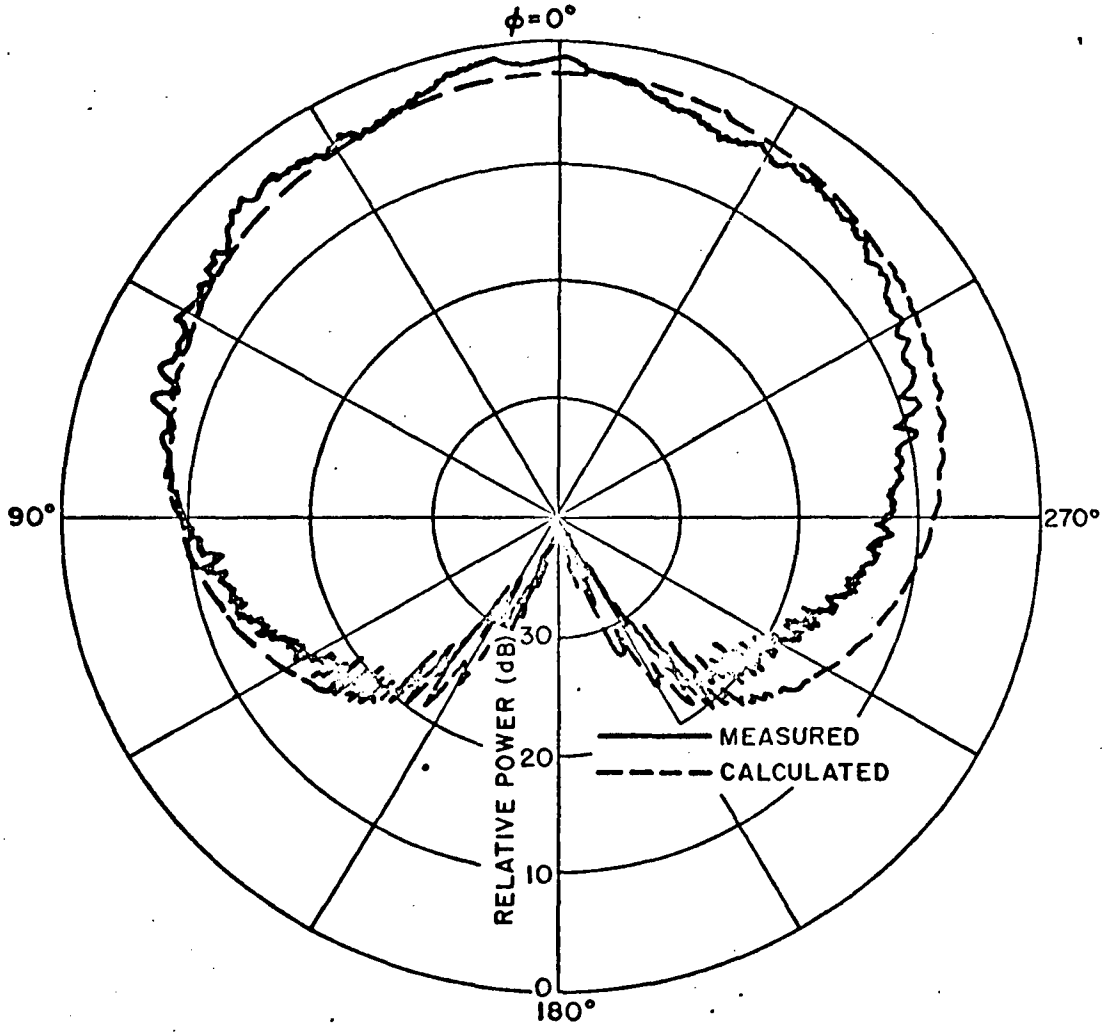

Fig. 24. Azimuth plane pattern of a $\lambda/4$ monopole mounted at station 220 on top of a Boeing 737 aircraft. (θ = 110°.)

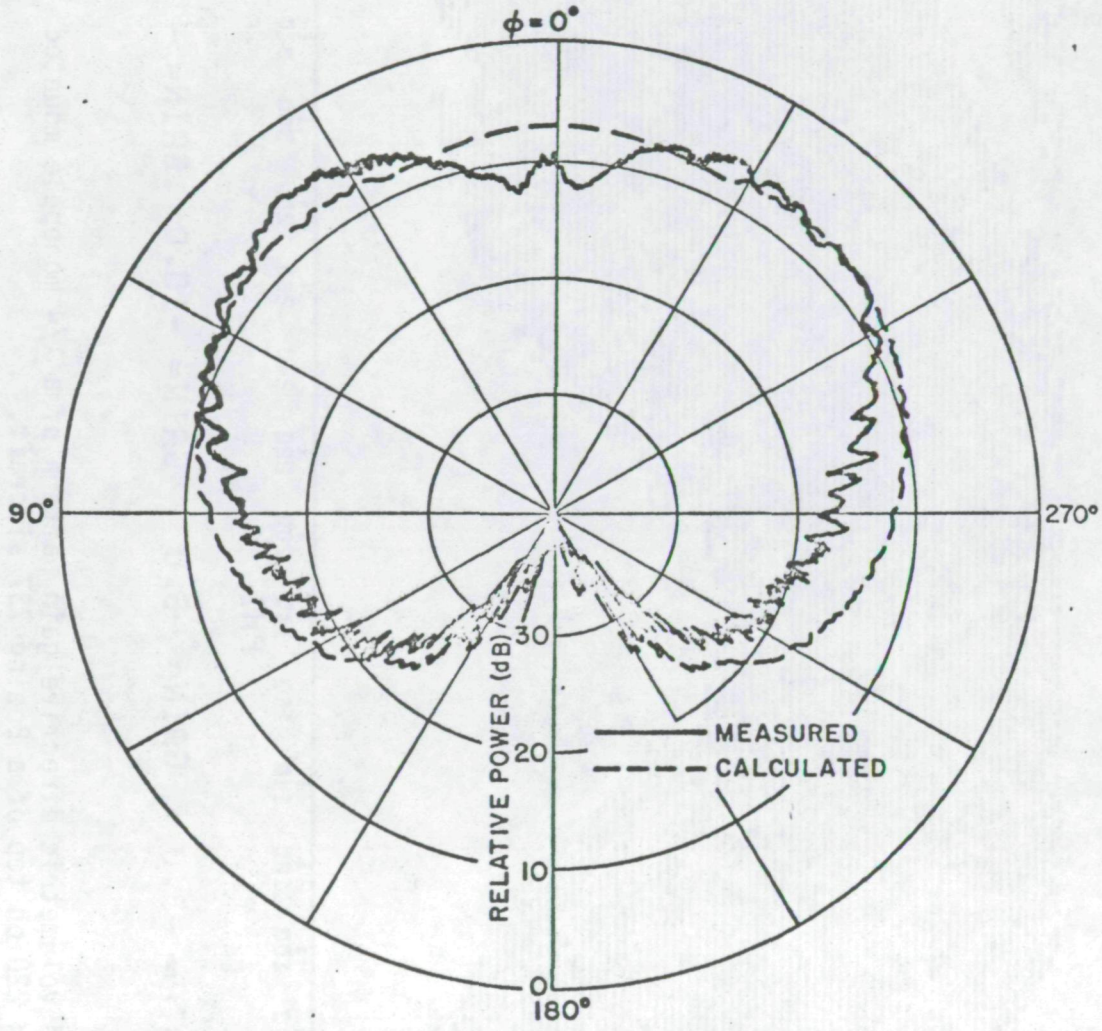

Fig. 25. Azimuth plane pattern of a λ/4 monopole mounted at station 220 on top of a Boeing 737 aircraft. (θ = 120°.)

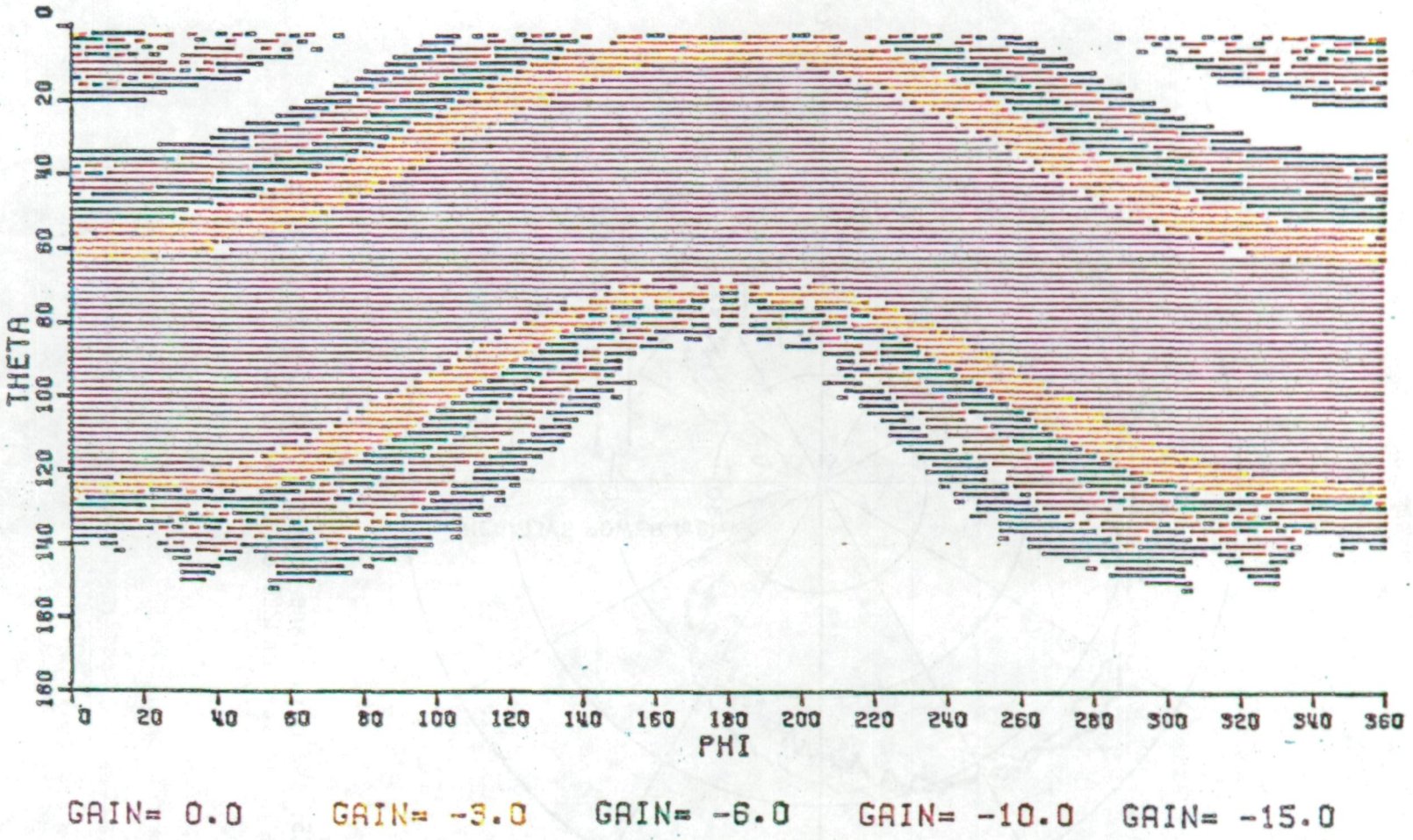

Fig. 26. Calculated volumetric directive gain pattern of a λ/4 monopole mounted at station 220 on top of a Boeing 737 aircraft.

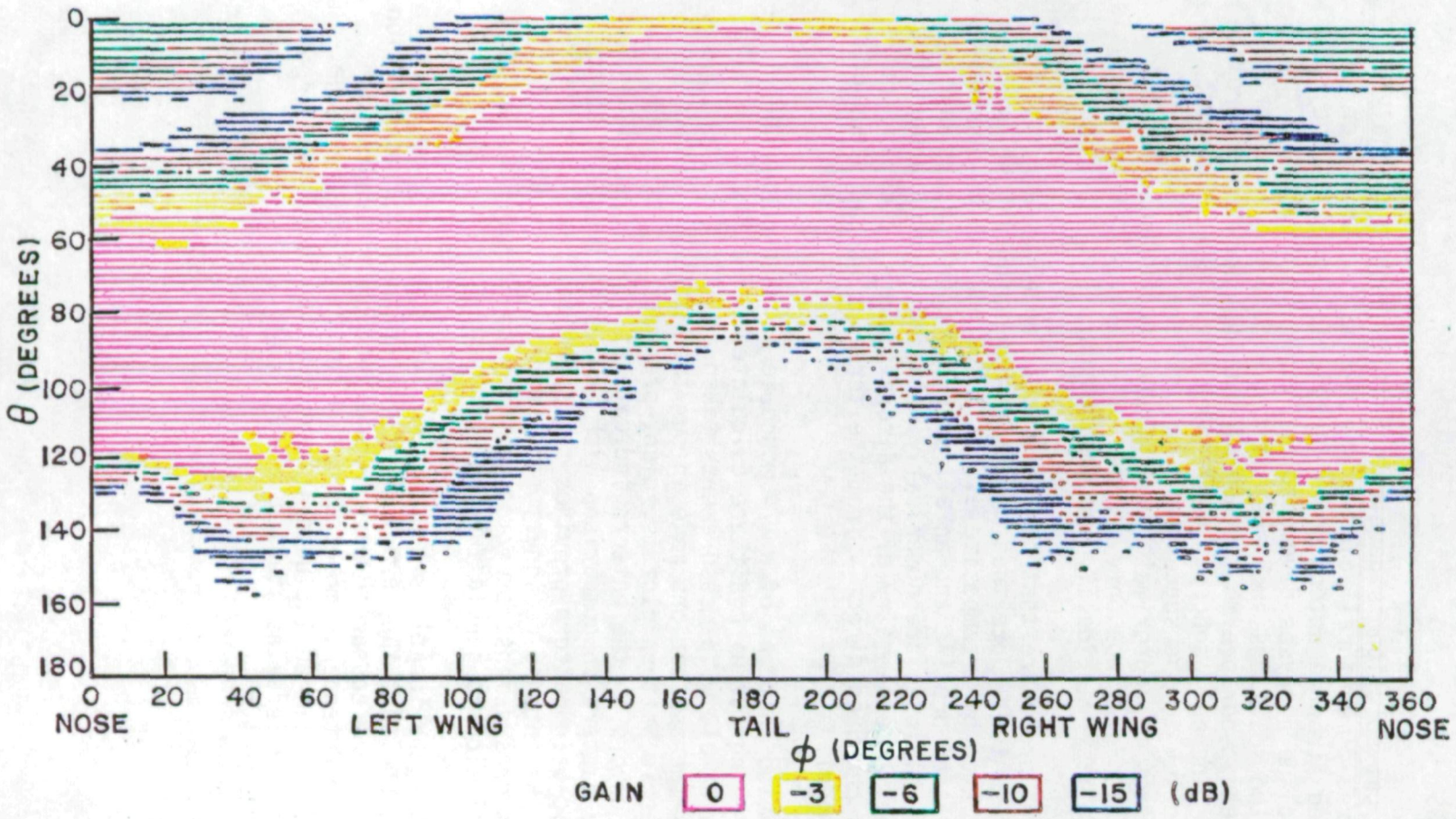

Fig. 27. Measured volumetric directive gain pattern of a λ/4 monopole mounted at station 220 on top of a Boeing 737 aircraft. This result was performed at NASA (Hampton, Va.).

IV. CONCLUSIONS

A theoretical solution is developed in this report to analyze complicated three-dimensional volumetric radiation patterns for fuselage mounted airborne antennas. This solution utilizes the roll and elevation plane analyses developed earlier. The procedure to combine these two solutions such that it can handle the volumetric pattern is based on our previous study of antennas mounted on prolate spheroids [2]. The belt concept in blending these two solutions together is the key to the success of the complete solution. The use of flat plates to approximate an aircraft cockpit and vertical stabilizer is also new; not only because of its simplicity in analysis but also due to its practicality in computation.

A numerical procedure that can be used to model an aircraft fuselage is presented. Note that the three-dimensional fuselage needed is simulated by a composite elliptic cylinder which approximates its elevation profile and an elliptic cylinder for its cross-section. These ellipses are numerically obtained through a best fit ellipse routine. The geometry of the aircraft wings, cockpit, and stabilizers is measured directly from the three principal views of the aircraft model.

The radiation patterns of a $\lambda/4$ monopole mounted above the cockpit on a Boeing 737 aircraft are calculated. The results are shown to compare well with measurements taken at NASA (Hampton, Va.), which verifies the assumptions made in our theoretical solutions. A color volumetric pattern plot is, also, presented in this report. The different colors in the pattern indicate different gain levels of the antenna pattern in comparison with an isotropic point source. This volumetric gain pattern provides the space coverage diagram necessary for the antenna designer. The success in predicting the volumetric patterns demonstrates the validity and capability of our theoretical solution to handle fuselage mounted airborne antennas.

For the antenna locations considered, the effect of the engines is negligible such that they are ignored in our present consideration. However, the engines appear to have some effect on the radiation patterns when an antenna is mounted on the bottom of the fuselage. The engine effect will be included in our computer model using a finite elliptic cylinder as studied in Ref. [6].

REFERENCES

1. Yu, C. L., and Burnside, W. D., "MLS Airborne Antenna Research," Semi-Annual Report 2902-22, May 1975, The Ohio State University ElectroScience Laboratory, Department of Electrical Engineering; prepared under Grant NGL 36-003-138 for National Aeronautics and Space Administration, Hampton, Virginia.

2. Burnside, W. D., "Analysis of On-Aircraft Antenna Patterns," Report 3390-1, August 1972, The Ohio State University ElectroScience Laboratory, Department of Electrical Engineering; prepared under Contract N62269-72-C-0354 for Naval Air Development Center. (AD 777 989)

3. Marhefka, R. J., and Burnside, W. D., "Numerical Solutions to Some On-Aircraft Antenna Pattern Problems," Technical Report 3390-4, October 1973, The Ohio State University ElectroScience Laboratory, Department of Electrical Engineering; prepared under Contract N62269-72-C-0354 for Naval Air Development Center.

4. Burnside, W. D., Gilreath, M. C., Marhefka, R. J., and Yu, C. L., "A Study of KC-135 Aircraft Antenna Patterns," IEEE Trans. on Antennas and Propagation, Vol. AP-23, No. 3, May 1975, pp. 309-316.

5. Jordon, E. C., and Balmain, K. G., Electromagnetic Waves and Radiating Systems, Prentice-Hall, Inc., New Jersey, 1968, p. 375.

6. Pathak, P. H., and Burnside, W. D., "An Asymptotic Result for the Scattering of Plane Waves by a Circular Cylinder," Report 3973-1, March 1976, The Ohio State University ElectroScience Laboratory, Department of Electrical Engineering; prepared under Contract N62269-74-C-0788 for Naval Air Development Center.

APPENDIX I

The necessary input data for the computer program which calculates the volumetric pattern of basic fuselage-mounted airborne antennas such as infinitesimal slot and monopole or $\lambda/4$ monopole are presented here for reference purposes. The following Read statements as required in the computer program are listed and explained so that the user is able to use and run the computer program.

```
READ(5,*)LWRT,LPLT,LBENT,LWING,LCOCK
READ(5,*) AR,BR,CR,AE,BE,CE,FRQG
READ(5,*)MS,MPR,MPE
READ(5,*) (JANTP(I),BETAP(I),PHSOP(I),ZSP(I),WM(I),WP(I), I=1,MS)
READ(5,*)(NXR(I),I=1,MPR)
READ(5,*)(MXFR(I),I=1,MPR)
READ(5,*) ((WGR(I,M,N),N=1,3),M=1,MXR)
READ(5,*) MBCR(I,1),MBCR(I,2),BPAR(I)
READ(5,*)(NXE(I),I=1,MPE)
READ(5,*)(MXFE(I),I=1,MPE)
READ(5,*) ((WGE(I,M,N),N=1,3),M=1,MXE)
READ (5,*) MBCE(I,1),MBCE(I,2),BPAE(I)
READ(5,*)ITHI,ITHF,ITHS,IPHI,IPHF,IPHS
READ(5,*) THC,PHC
READ(5,*) RADC,DBLV,IPLT,IPLTP,ICWP,IWRITE,IWRT
```

LWRT: Additional write out desired (True or False)?
LPLT: Radiation pattern plotted by pen plotter desired? (T or F)
LBENT: The input data for the bent plate geometry has been bent (T) or not (F).
LWING: Is there any wing or horizontal stabilizer attached to roll plane cylinder (T) or not (F)?
LCOCK: Is there any radome nose-section (approximated by flat plate) or/and vertical stabilizer (T) or not (F)?

All input dimensions in inches or degrees and the last letter R or E on each variable indicates roll plane elliptic cylinder model or elevation plane composite elliptic cylinder model.

AR = X-dimension of fuselage cross-section ***
BR = Y-dimension of fuselage cross-section ***
CR = -Y-dimension of fuselage cross-section ***
AE = X-dimension of fuselage profile ***
BE = Y-dimension of fuselage profile ***
CE = -Y-dimension of fuselage profile ***
FRQG = Frequency in GHz.
MS = Number of sources ***.

MPR: number of wings and horizontal stabilizers in roll plane elliptic cylinder

MPE: number of nose section flat plate and vertical stabilizer. Attached on elevation plane elliptic cylinder (or no. of corners or edges per plate).

JANTP: array of antenna type (infinitesimal element) slot = 1; radial monopole = 2, radial 1/4 wavelength monopole = 3.

BETAP: the angle of the array of slot elements make with z axis.

PHSOP: the angular position of the antenna elements in fuselage cross section.

ZSP: the z coordinate of source elements relative to reference coordinate system.

the magnitude of the source elements.

WP: the phase of the source elements.

NXR,NXE: the number of corners in each plate (wings of stabilizers).

MXFR(I) = the sign of this array indicates whether the last corner of the plate is attached to the fuselage( ) or not (-). The content of the array is the number of last corner (MX).

WGR,WGE: the XYZ coordinates of the corners of each plate in roll plane or elevation plane models. The coordinates are in terms of roll plane model or elevation plane model respectively. One point represents the XYZ component of a corner of the wing points must be ordered counterclockwise. WGR(I,M,N) The first point being on the fuselage
I : the plate number.
M : the corner number.
N : the XYZ coordinates.

MBCR(I,J): I = the plate number.
J: 1 = first corner of the bent plate.
2 = last corner of the bent plate.

BPAR(I) = the angle between two plates.

ITHI,IPHI = initial value of theta and phi in degrees where theta and phi are the radiaiton angles.

ITHF,IPHF = final value of theta and phi in degrees

ITHS,IPHS = incremental step in theta and phi in degrees

THC,PHC = theta and phi and the rotation angles of the axis of pattern rotation. Note that ITHI,ITHF are the initial and final values in rotated coordinate system.

RADC = size in inches of the desired plot.

DBLV = the dB level to be normalized.

IPLT = type of plot desired. If IPL T = 1 field plot

IPLT = 2 power plot ***** IPLT = 3 dB plot.

IPLTP: indicates whether E-theta or E-phi or both pattern to be plotted. If IPLTP lies between 0 & -5; the pattern can be replotted with different radius. If IPLTP less than -5: then the program continues on for next set of data.

ICWP: indicates the pattern plot is in C.W.(+) or C.C.W.(-) sense.

IWRITE: indicates output from the plot package to be written out (+) or not (-).

IWRT: indicates whether various output to be written out.

MPLT = the number of the sets of data to be plotted.

The following sample data is for a $\lambda/4$ monopole mounted on station 220 on top of a Boeing 737 aircraft. The elevation plane radiation pattern is desired in this case. These data are read in free formats into the computer for convenience. If no free format is allowed in a particular computer, there are also fixed read formats in the program which are added as common cards at present.

```
 1    F,T,T,T,T
 2    65,86,+43.3,58.72,308.56,1307.04,3.18
 3    1,2,2
 4    3,0.,0.,-278.,1.,0.
 5    4,4
 6    4,4
 7    0.,43.3,56.54
 8    0.,536.93.316.14
 9    0.,536.93,379.86
10    0.,43.3,233.54
11    4,4,180.
12    0.,-43.3,233.54
13    0.,-536.93,379.86
14    0.,-536.93,316.14
15    0.,-43.3,56.54
16    4,4,180.
17    4,4
18    4,4
19    0.,308.56,-31.585
20    -5.6,321.6,-27.07
21    -5.6,321.6,27.07
22    0.,308.56,31.585
23    4,4,180.
24    54.645,-478.4,8.25
25    284.147,-683.696,8.25
26    284.147,-683.696,-8.25
27    54.645,-478.4,-8.25
28    4,4,180.
29    90,91,5,0,360.2
30    90.,-90.
31    3.75,0.,3,3,1,1,3
```